



1 Differences in MOPITT surface-level CO retrievals and trends from Level 2 and Level 2 3 products in coastal grid boxes

3

4 Ian Ashpole¹ and Aldona Wiacek^{1,2}

5

6 ¹Department of Environmental Science, Saint Mary's University, Halifax, Canada

7 ²Department of Astronomy and Physics, Saint Mary's University, Halifax, Canada

8 Correspondence to: Ian Ashpole (ian.ashpole@smu.ca)

9

10

11 Abstract

12

13 MOPITT retrievals are more sensitive to near-surface CO when performed over land than water. Data users
14 are therefore advised to discard retrievals performed over water from analyses to limit the a priori influence
15 on results. Level 3 (L3) products are a 1° x 1° gridded average of finer resolution Level 2 (L2) retrievals. For
16 coastal grid boxes, these are retrievals that are either performed over land, water, or a combination of the
17 two, on any given day. L3 data users therefore have limited ability to filter for retrievals performed over
18 water for these grid boxes. The consequences that this has on retrievals and their temporal trends in “as-
19 downloaded” L3 data (L3O) are examined in this paper, for all coastal L3 MOPITT grid boxes (n = 4299),
20 by comparison to separate land- and water-only grid box averaged L2 retrievals (L3L and L3W, respectively).
21 First, it is established that mean retrieved VMRs in L3L and L3W differ by over 10 ppbv, significant (p <
22 0.1) at 60 % of the coastal grid boxes. Trends are also stronger in L3L (mean difference between 0.28 ppbv
23 y⁻¹ and 0.43 ppbv y⁻¹), with the L3L – L3W trend difference significant at 36 % of grid boxes. These L3L-
24 L3W differences are clearly linked to retrieval sensitivity differences, with L3W being more heavily tied to
25 the a priori CO profiles used in the retrieval, which is a model-derived monthly mean climatology. On days
26 when L3O is created from the averaging together of L2 retrievals over both land and water (L3O_M), the result
27 is VMRs that are significantly different to L3L for 75 % of grid boxes where the L3L – L3W difference is
28 also significant, 45 % of all coastal grid boxes. Just under half of the grid boxes that featured a significant
29 L3L – L3W trend difference also see trends differing significantly between L3L and L3O_M. Factors that
30 determine significance of difference between L3O_M and L3L include proportion of the surface covered by
31 land/water, and the magnitude of sensitivity contrast. Comparing the full L3O dataset to L3L, it is shown that
32 if L3O is filtered so that only retrievals over land (L3O_L) are analysed, there is a huge loss of days with data.
33 This is because L2 retrievals over land are routinely discarded during the L3O creation process, for coastal
34 grid boxes. The problem can be lessened by also retaining L3O_M retrievals, but the resulting L3O “land or



35 mixed” (L3O_{LM}) subset still has less data days than L3L for 61 % of coastal grid boxes. Moreover, as already
36 shown, these additional days with data feature some influence from retrievals made over water that can affect
37 results. Coastal L3 grid boxes contain 33 of the 100 largest coastal cities in the world, by population. Focusing
38 on the L3 grid boxes containing these cities, it is shown that mean VMRs in L3O_L and L3L differ significantly
39 for 11 of the 27 cities that can be compared (there are no L3O_L data for 6 of the cities). The L3L – L3O_{LM}
40 mean VMR difference exceeds 10 (22) ppbv for 11 (3) of the 33 cities, significant in 13 cases. 9 of the 18
41 cities where WLS analysis can be performed in L3O_L feature a trend that is significantly different to L3L.
42 The trends in L3O_{LM} and L3L differ significantly for 5 of the 33 cities. It is concluded that a L3 product
43 based only on L2 retrievals over land would be of benefit to MOPITT data users, given the clear and
44 sometimes significant differences in mean CO VMRs and trends that can be obtained for coastal grid boxes
45 using L2 products in which retrievals performed over water can be more easily discarded.

46

47

48 **1. Introduction**

49

50 Carbon monoxide (CO) is directly emitted into the atmosphere from anthropogenic (e.g. fossil fuel burning)
51 and natural (e.g. wildfire) sources, and also produced via the oxidation of hydrocarbons in the atmosphere.
52 With an atmospheric lifetime of weeks to months (e.g. Duncan et al., 2007), it is an important tracer of
53 pollutant transport and indicator of emission sources. While a health concern in its own right at high enough
54 concentrations, CO also plays an important role in atmospheric chemistry, for example as a precursor to
55 ozone formation and a primary sink for the hydroxyl radical. Atmospheric CO concentrations have decreased
56 since the start of the 21st century, with a slowdown in the rate of decline observed in recent years (Buchholz
57 et al., 2021). Trends also show substantial spatial variability (Hedelius et al., 2021). Satellite instruments
58 have been central to our understanding of global change in CO concentrations, with the Measurement of
59 Pollution in the Troposphere (MOPITT – Drummond et al., 2010, 2016) instrument well suited to this task,
60 providing a nearly-unbroken and consistent data record since the year 2000.

61 MOPITT observes upwelling radiances at thermal infrared (TIR) and near infrared (NIR) wavelengths
62 and uses these in an optimal estimation retrieval algorithm to retrieve coarse vertical resolution CO profiles,
63 which are integrated to give total column amounts. Among multiple additional inputs required by the retrieval
64 algorithm, a priori CO profiles – which describe the most probable state of the CO profile at a given location
65 – are necessary to constrain the retrieval to physically reasonable limits (Pan et al., 1998; Rodgers, 2000; the
66 retrieval algorithm is outlined in more detail in Sect. 2.1). For the most recent iterations of MOPITT products,
67 these a priori CO profiles are based on a monthly climatology from a chemical transport model. The degree
68 to which a given MOPITT retrieval reflects information obtained from the observed radiances – known as



69 “information content” – is highly spatially and temporally variable, depending on scene-specific factors such
70 as surface temperature, thermal contrast in the lower troposphere, and the actual (“true”) CO loading itself,
71 as well as on instrumental noise (e.g. Deeter et al., 2015). The lower the retrieval information content, the
72 closer the retrieved CO loading will be to the a priori; a model value.

73 Retrievals that take place over water are known to have a lower information content than retrievals
74 that take place over land. This is due to weak thermal contrast near to the surface hampering the instrument’s
75 ability to sense CO absorption in the lowermost layers of the troposphere (Deeter et al., 2007; Worden et al.,
76 2010). It is therefore recommended that MOPITT data users exclude these retrievals from any analyses they
77 perform, to ensure that results are not biased by retrievals that have a heavy reliance on the a priori (MOPITT
78 Algorithm Development Team, 2018; Deeter et al., 2015). Such filtering is specifically emphasised where
79 the focus of analysis is the identification of long-term CO trends, because any real trends in the data will be
80 weakened by the inclusion of retrievals that are tied heavily to the a priori (Deeter et al., 2015). This is
81 because the a priori CO profiles are taken from monthly modelled CO climatologies: for a given location and
82 day of the year, they will be the same every year and therefore feature no temporal trend (Deeter et al., 2014).

83 MOPITT data are available as either Level 2 (“L2”) or Level 3 (“L3”) products. L2 products contain
84 each individual retrieval, at ~22 x 22 km spatial resolution. L3 products are a 1° x 1° gridded area-average of
85 the individual L2 retrievals that fall within each grid box (see Fig. 1), with some filtering criteria applied.
86 One criterion is the surface type over which the L2 retrievals were performed – either land, water, or “mixed”.
87 If more than 75 % of the bounded L2 retrievals were performed over the same surface type then only those
88 retrievals are averaged to create the L3 product and the rest are discarded; otherwise, all bounded L2 retrievals
89 are averaged, and the L3 product is given the surface type classification of “mixed” (L3 surface type
90 classification is explained in more detail in Sect. 2.2). This creates a problem for L3 grid boxes that overlay
91 coastlines: To a greater or lesser extent, these L3 products will have some contribution from L2 retrievals
92 performed over water, as shown in Fig. 1. L3 product users have limited capability to discard them, at least
93 without sacrificing temporal resolution (because each L3 grid box only has a single retrieval per day). By
94 contrast, with L2 products it is possible, for the same coastal grid boxes, to choose to retain only the retrievals
95 performed over land. In practical terms, this means that, for coastal L3 grid boxes, valuable retrieval
96 information over land, available in L2 products, can be lost to users of L3 products.

97 With a focus on the coastal L3 grid box containing the city of Halifax, Canada, Ashpole and Wiacek
98 (2020) demonstrate the consequences of this loss of retrieval information in L3 products. They compare the
99 results of analyses performed using L3 data and L2 data whereby only bounded retrievals performed over

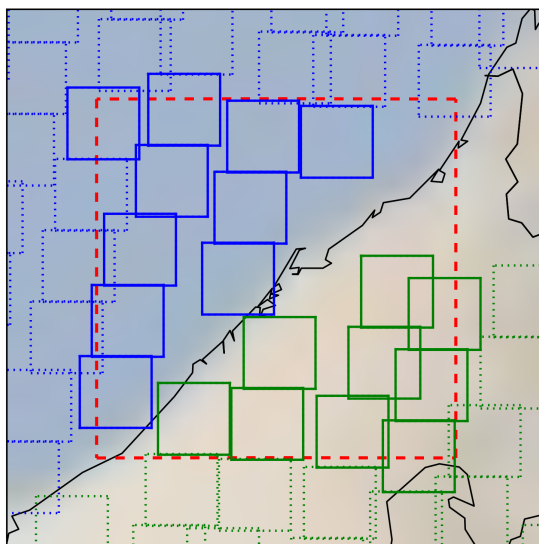


Figure 1. Example of coastal L3 grid box (red dashed box) and bounded L2 retrievals from which the L3 products for that grid box are created. Blue (green) boxes correspond to L2 retrievals with a surface index of “water” (“land”). Note that only L2 retrievals with a midpoint that falls within the boundaries of the L3 grid box will be used in L3 creation for that grid box. These are indicated by solid blue/green outlines – those not included in L3 creation for this grid box are shown with dotted blue/green outlines. More information on surface indexing and L3 product creation is given in Sect. 2.2. “Coastal” L3 grid box classification is outlined in Sect. 2.3. The coastal L3 grid box visualized here contains the city of Dubai (~centre = 55.296° E, 25.277° N), which features in the case study analysis of Sect 3.4. Background shading is from Nasa Blue Marble imagery.

100 land were retained, and find significant differences in both seasonal mean statistics and the magnitudes of
101 trends identified in surface-level CO. These differences are a direct result of the L3 products being dominated
102 by L2 retrievals over water, which feature a weaker trend than the L2 retrievals over land, demonstrably due
103 to a greater a priori influence owing to their reduced true-profile sensitivity. In their conclusions, Ashpole
104 and Wiacek (2020) suggest that L2 retrievals over water should not contribute to L3 products for coastal grid
105 boxes, which would be consistent with previous data filtering recommendations (MOPITT Algorithm
106 Development Team, 2018; Deeter et al., 2015). The primary aim of this paper is to explore the extent of the
107 difference that this would make on a global scale. This is necessary to understand for two reasons: firstly, L3
108 data are better suited to long timeseries analysis than L2 data owing to their smaller file size (~25 MB vs
109 ~450 MB respectively, for a single daily, global file). It cannot be overlooked that working with L3 data thus
110 requires fewer computing resources and less technical proficiency. L3 products thus make the MOPITT data
111 more easily accessible, especially to less-expert users, who may lack the expertise required to scrutinize the
112 data for potential a priori bias. Secondly, many of the world’s largest agglomerations are situated within a



113 coastal L3 grid box (5 of the top 10 and 33 of the top 100 largest agglomerations by population; derivation
114 outlined in Sect. 2.5), making these likely targets for analyses of air quality indicators, especially their
115 changes over time.

116 This paper presents a comparison of results from analyses performed using L3 data products and
117 separate land-only and water-only area averages from L2 products for all MOPITT L3 grid boxes that overlay
118 coastlines. Section 3.1 demonstrates the magnitude of the sensitivity difference for retrievals over land and
119 water, zooming in to focus on coastal grid boxes, the classification of which is outlined in Sect. 2.3. Section
120 3.2 links the sensitivity contrast to differences in mean CO volume mixing ratios and their temporal trends
121 for L2 retrievals performed over land and water within coastal L3 grid boxes, and evaluates the effect that
122 the averaging together of these retrievals has on the statistics and trends in resulting L3 “mixed” values.
123 Section 3.3 quantifies the proportion of L2 retrievals performed over land within coastal L3 grid boxes that
124 are lost to L3 products, before finally comparing statistics and trends in L3 and L2 products for all coastal
125 L3 grid boxes, outlining the magnitude and significance of differences for the 33 largest coastal cities in the
126 world (Sect. 3.4).

127

128

129 **2. Data and Methods**

130

131 **2.1. MOPITT Instrument and retrieval overview**

132

133 Carried on board the polar-orbiting NASA Terra satellite that was launched in December 1999, MOPITT
134 began measuring CO in March 2000 and has provided near-continuous measurements to date. With a native
135 pixel resolution of $\sim 22 \times 22$ km at nadir and a swath width of ~ 640 km, it offers near global coverage roughly
136 every 3-days, crossing the equator at $\sim 10:30$ and $\sim 22:30$ local time. The instrument is a gas correlation
137 radiometer that measures radiances in two CO-sensitive spectral bands: the TIR at $4.7 \mu\text{m}$, which is sensitive
138 to both absorption and emission by CO and can provide information on its vertical distribution in the
139 troposphere; and the NIR at $2.3 \mu\text{m}$, which constrains the CO total column amount and yields information
140 on CO concentrations in the lower troposphere (LT), to which TIR radiances are typically less sensitive
141 (Drummond et al., 2010; Pan et al., 1995, 1998). For the work presented here, the TIR-NIR combined
142 MOPITT product is used, owing to its demonstrably greater sensitivity to CO loadings near to the surface
143 than the TIR- and NIR- only products which are also available (Deeter et al., 2013). Note, however, that
144 retrievals over water and at night are limited to the TIR band only due to the lacking NIR signal. This analysis
145 is based on daytime-only retrievals (more information on data selection and preparation is given in Sect. 2.4).



146 Multiple other sources describe the retrieval algorithm in detail (e.g., Deeter et al., 2003; Francis et
147 al., 2017). In short, it uses optimal estimation (Pan et al., 1998; Rogers, 2000) and a fast radiative transfer
148 model (Edwards et al., 1999) to invert measured radiances and retrieve the CO volume mixing ratio (VMR)
149 profile on 10 vertical layers. The vertical grid consists of 9 equally spaced pressure levels from 900 to 100
150 hPa (the uppermost level covers the atmospheric layer from 100 to 50 hPa), with a floating surface pressure
151 level (if the surface pressure is below 900 hPa, less than 10 profile levels are retrieved). Retrieved values
152 represent the mean CO VMR in the layer immediately above that level. These profile measurements are then
153 integrated to provide total column CO amounts. Retrievals are only performed for scenes free of cloud (cloud
154 clearing is based on coincident MODIS observations and MOPITT's own radiances).

155 In addition to the measured radiances, the retrieval requires multiple inputs including meteorological
156 data, surface temperature and emissivity, and, of direct relevance to this study, a priori CO profiles, which
157 are necessary to constrain the retrieval to physically reasonable limits. These a priori CO profiles come from
158 a monthly CO climatology (years 2000-2009), simulated with the Community Atmosphere Model with
159 Chemistry (CAM-chem) chemical transport model (Lamarque et al., 2012) at a spatial resolution of 1.9° x
160 2.5°, which is then spatially and temporally interpolated to the time and location of each individual MOPITT
161 observation. A priori profiles for a given location and day of the year are therefore the same every year and
162 feature no temporal trend. To understand the physical significance of the MOPITT CO retrievals, it is
163 necessary to examine the retrieval Averaging Kernels (AKs), available with all MOPITT data products,
164 which quantify the sensitivity of the retrieved vertical profile to the “true” vertical profile. The lower the
165 retrieval sensitivity, the greater the a priori weighting. Two different components of AKs are analysed in this
166 paper: AK rowsums, which represent the overall sensitivity of the retrieved profile at the corresponding
167 pressure level to the whole true profile; and AK diagonal values, which represent the sensitivity of the
168 retrieved profile at the corresponding pressure level to the same level of the true profile (e.g. the AK diagonal
169 value for the surface level of the retrieved profile represents its sensitivity to the surface level of the true
170 profile).

171 From time-to-time, new MOPITT products become available as improvements are made to the
172 retrieval algorithm and radiative transfer model, yielding superior validation statistics compared to earlier
173 product versions (Worden et al., 2014). This analysis uses MOPITT Version 8 (V8) products (Deeter et al.,
174 2019). Note that Version 9 (V9) products became available shortly after this study was completed. V9
175 features cloud screening improvements that yield additional retrievals over land in comparison to V8 (the
176 exact percent change varies significantly with geography). Validation results are comparable to V8. It is
177 expected that the main conclusions of this paper to hold for V9, since the land-water sensitivity contrast



178 remains and L3 processing method appears to be unchanged. An overview of MOPITT V9 is given by Deeter
179 et al (2021).

180

181

182 **2.2. MOPITT surface type classification**

183

184 To aid in filtering and interpreting retrievals, all MOPITT data products are distributed with a range of
185 diagnostic fields. As retrieval information content is known to be variable depending on the type of surface
186 over which it is performed (Deeter et al., 2007), L2 retrievals are given a surface index according to whether
187 they were performed over land, water, or a combination of the two (“mixed”). For a given $1^\circ \times 1^\circ$ L3 grid
188 box, how the L2 retrievals that fall within its boundaries are processed to produce the L3 product depends on
189 how their surface indexes vary: If more than 75 % of the bounded L2 retrievals have the same surface index,
190 only those retrievals are averaged to produce the L3 gridded value, and the L3 surface index is set to that
191 surface type (the other L2 retrievals are discarded). Otherwise, all L2 retrievals available in the L3 gridbox
192 are averaged together and the L3 surface index is set to “mixed”, as is the case in the example shown in Fig.
193 1 (this information is taken from the MOPITT Version 6 L3 data quality summary¹, which at the time of
194 writing, is the most recent data quality summary to detail exactly how L3 data are created). Note that the L2
195 VMR profiles that are averaged to produce the L3 retrieval are first converted to $\log(\text{VMR})$ profiles, then
196 averaged, and the mean $\log(\text{VMR})$ profile is then converted back to a VMR profile.

197 Each L3 grid box only has one retrieval per day. This dictates that where the grid box overlies both
198 land and water, its surface index will vary through time, depending on the population of L2 retrievals from
199 which it is created. The make-up of this population can also vary from day-to-day due to factors such as cloud
200 cover, and screening for data quality issues: on day n the population could be predominantly L2 retrievals
201 over land, on day $n+1$ it could be predominantly L2 retrievals over water, and on day $n+2$ it could be an even
202 mix of the two. Given that the averaging together of retrievals with significantly different sensitivity profiles
203 – as could be the case when averaging retrievals over land and water – serves to dilute the information coming
204 from the MOPITT observed radiances with information coming from the a priori and is therefore discouraged
205 (MOPITT Algorithm Development Team, 2018; Deeter et al., 2015; Deeter et al., 2007); and that MOPITT
206 data users are advised to exclude retrievals over water from analyses owing to the known reduced sensitivity,
207 this introduces two potential problems for L3 data taken from coastal grid boxes: firstly, discarding all L3
208 retrievals with the surface index of water will result in a loss of temporal coverage; secondly, L3 retrievals

¹ available here: https://eosweb.larc.nasa.gov/sites/default/files/project/mopitt/quality_summaries/mopitt_level3_ver6.pdf



209 with a surface index of mixed feature some contribution from L2 retrievals over water. The consequences of
210 both of these problems are explored in this paper.

211

212

213 **2.3. Coastal grid box classification for this study**

214

215 Since the focus of this paper is on “coastal” L3 grid boxes, it is first necessary to isolate these from the
216 remaining “land-only” or “water-only” L3 grid boxes in the MOPITT data set. The initial step is to identify
217 all grid boxes that have a surface index of “mixed” at least once during the study period. This indicates that
218 the ground area within those grid boxes was both land and water. However, analysis of the global distribution
219 of L3 grid boxes featuring a surface index of mixed revealed that, in addition to actual coastlines, a large
220 proportion of inland grid boxes that are clearly not coastal (“false coastal”) are given the surface index of
221 mixed at least some of the time (Fig. 2a). The reason for this is unclear, but it could be for real physical
222 reasons, such as land grid boxes sporadically flooding, or due to issues in the retrieval schemes caused by
223 e.g. cloud screening problems or the presence of surface ice cover. One characteristic of these false coastal
224 grid boxes is that, compared to the total number of days with L3, the relative frequency with which they are
225 flagged as land is very high (expressed as the ratio “n_days(L3O_L/L3O)”, plotted in Fig. 2b). This relative
226 frequency is much lower for “true” coastal grid boxes, to be expected given prior knowledge of 1) the fact
227 that these grid boxes span both land and water surface types; and 2) how the surface index is determined for
228 L3 data (as outlined in Sect. 2.2). Following iterative threshold testing, L3 coastal grid boxes are classified
229 as grid boxes that:

230

231 1. Have at least one classification of “mixed” during the study period

232 2. Have an n_days(L3O_L/L3O) ratio < 0.5.

233

234 The distribution of coastal grid boxes identified using these criteria is shown in Fig. 2c. Most false coastal
235 grid boxes are removed, although there are still some erroneous classifications evident, mostly in the north
236 of Canada and Russia. However, placing a more restrictive threshold on the n_days(L3O_L/L3O) ratio to
237 remove these areas has diminishing returns since it results in the rejection of more true coastal grid boxes.
238 These criteria therefore strike a balance between minimising false and maximising true classifications.

239 Applying these criteria to the MOPITT L3 data yields 4299 coastal grid boxes, from a total of 64800
240 L3 grid boxes (6.6 %). This mask is applied to all data, and only those L3 grid boxes that remain are classified

241 as coastal. Only data for these coastal grid boxes are analysed in this study (with the exception of global L3
242 maps in Sect. 3.1.1).

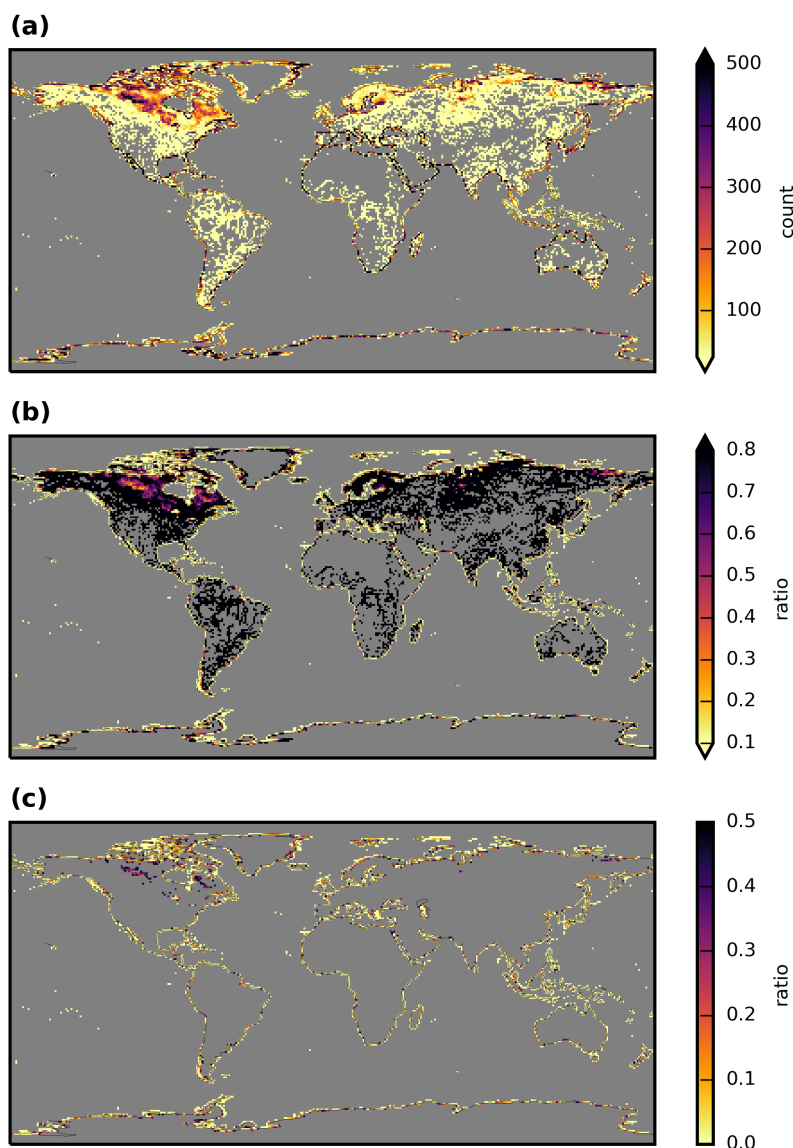


Figure 2. Maps showing the stages of derivation of the coastal L3 grid box mask applied in this paper to MOPITT data. **(a)** Frequency with which L3 grid boxes are given the surface index of “mixed”, calculated from daily data between 2001-08-25 and 2019-02-28. **(b)** Frequency with which L3 grid boxes that have a surface index of “mixed” at least once in panel a have the surface index of “land”, compared to the total number of days with which L3 data are available for that grid box (expressed as $n_days(L3O_l/L3O)$). **(c)** As b, but with a threshold of $n_days(L3O_l/L3O) < 0.5$ applied. This is the coastal L3 grid box mask used in this paper.



243 2.4. MOPITT datasets analysed, and data processing methods

244

245 All available MOPITT V8 Level 2 (L2) and Level 3 (L3) TIR-NIR files (“MOP02J” and “MOP03J” files,
246 respectively) were downloaded from the NASA Earthdata portal (<https://search.earthdata.nasa.gov>).
247 Although the data record begins in March 2000, analysis is restricted to the period from 2001-08-25 to 2019-
248 02-28. Data prior to 2001-08-25 are discarded due to an instrumental reconfiguration in 2001 creating an
249 inconsistency in the data record (Drummond et al., 2010). Data post 2019-02-28 are flagged as “beta” at the
250 time of writing, their use in scientific analysis (especially for examining long-term records of CO) being
251 discouraged until final processing and calibration occurs (MOPITT Algorithm Development Team, 2018).
252 For clarity, the original, “as-downloaded” L3 timeseries is referred to as “L3O” for the remainder of this
253 paper. Only retrievals that were performed during daytime hours are retained (daytime and nighttime
254 retrievals are stored as separate fields in MOP03J files). For this analysis, separate subsets of L3O are created
255 according to surface index: L3O land-only (“L3O_L”), L3O water-only (“L3O_W”), L3O mixed (“L3O_M”), L3O
256 land-or-mixed (“L3O_{LM}”). When the L3O dataset is analysed with no filtering by surface index applied, it is
257 referred to as “L3O_{NF}”.

258 The first step of L2 data processing for this study is to filter the retrievals as is done at the L3
259 processing stage. This involves:

260

- 261 • Discarding all observations for Pixel 3 (this corresponds to one of MOPITT’s four detectors);
- 262 • Discarding all observations where both (1) the channel 5A signal-to-noise-ratio (“SNR”) < 1000 and
263 (2) the channel 6A SNR < 400 (5A and 6A correspond to the average radiances for MOPITT’s length-
264 modulated cell TIR and NIR channels, respectively)

265

266 This filtering takes place because observations from specific elements on MOPITT’s detector array were
267 found to exhibit greater retrieval noise than the other elements, and their inclusion therefore lowered overall
268 L3 information content (MOPITT Algorithm Development Team, 2018). Only daytime L2 retrievals are
269 retained, using a solar zenith angle filter of < 80°.

270 From the remaining set of filtered L2 retrievals, separate area averages are taken for those with a
271 surface index of land and water, for every 1° x 1° L3 grid box. This effectively creates two new L3 “land
272 only” and “water only” products, which are referred to herein as “L3L” and “L3W”. For clarity of analysis,
273 remaining L2 retrievals with a surface index of mixed are discarded. These make up a very small proportion
274 of the overall L2 retrievals (e.g. < 5 % for the grid box containing Halifax, analysed in Ashpole and Wiacek,
275 2020). Note that, as with the creation of L3O, L2 VMR profiles for each L3 grid box are first converted to



276 log(VMR) profiles before averaging, and the mean log(VMR) profile is then converted back to a VMR profile
277 to give the final L3L and L3W retrievals.

278 From these L3O, L3L, and L3W datasets, only grid boxes that are classified as “coastal” using the
279 coastal grid box masked outlined in Sect. 2.3 are analysed.

280

281

282 **2.5. Statistical methods used for this study, and additional data sources**

283

284 For every coastal L3 grid box, two separate timeseries from each of the L3O, L3L, and L3W datasets are
285 analysed. In Sect. 3.1 and 3.2 the timeseries analysed only contain days where L3L and L3W are both present
286 and the L3O surface index is mixed (“L3O_M”). In Sect. 3.3 and 3.4 the full timeseries from each dataset is
287 analysed. Descriptive statistics are calculated from both timeseries across the whole study time period, and
288 also for individual years (full years only – 2002 to 2018 inclusive).

289 To identify and compare temporal trends for each coastal grid box in the datasets outlined above,
290 weighted least squares (WLS) regression analyses is performed on yearly mean values, weighted by the
291 inverse of the standard deviation of the measurements used in the yearly mean (i.e. $1/\sigma$). For years that contain
292 just a single retrieval, the weighting is set to $1/100000$ to de-weight them in the fit. If there are more than 2
293 years in a timeseries for a given grid box that have no data, the regression analysis is not performed. WLS is
294 preferred over OLS because it is less sensitive to outliers. For simplicity, no other trend detection methods –
295 e.g. the Thiel-Sen slope estimator – are applied to corroborate the trends that are detected with WLS. Such
296 extra steps would be necessary if the actual trend values were the focus of this study; however, the aim of
297 this trend analysis is instead to identify whether the same method can yield different results depending on
298 which of L3O, L3L or L3W is analysed.

299 To determine whether two trends identified are significantly different, their difference is evaluated
300 using the Z test as follows:

301

$$302 \quad Z = \frac{Trend_1 - Trend_2}{\sqrt{SE_1^2 + SE_2^2}}$$

303

304 where SE_1 and SE_2 correspond to the standard errors of $Trend_1$ and $Trend_2$ respectively, and Z is the test
305 statistic. Where Z is greater (less) than 1.645 (-1.645) the trend difference is statistically significant to at least
306 90 % (i.e. $p < 0.1$). In addition, two trends are classified as being significantly different if $Trend_1$ is



307 significantly different to zero ($p < 0.1$) but Trend_2 is not ($p > 0.1$), and vice-versa (i.e. the conclusion would
308 be that Trend_1 is not zero, but Trend_2 may be).

309 A list of the top 100 largest agglomerations by population in the world is obtained from
310 <http://www.citypopulation.de/> (valid at time of writing). 33 of these are situated in a coastal grid box,
311 according to the classification in Sect. 2.3. Time series of L3L, L3W, and L3O are extracted from each of
312 these grid boxes for the analysis in Sect. 3.4.

313

314

315 **3. Results and Discussion**

316

317 **3.1. Land-water contrast in MOPITT sensitivity**

318

319 This section demonstrates the land-water sensitivity contrast in MOPITT retrievals at levels throughout the
320 vertical profile, and examines the magnitude of the difference within coastal L3 grid boxes.

321

322

323 **3.1.1. Global context**

324

325 Figure 3 shows long-term mean maps for the retrieval sensitivity metrics AK diagonal value, AK rowsum,
326 and retrieved minus a priori VMR (“VMR ret-apr”) at selected profile levels, created from L3O data averaged
327 across the entire study period (September 2001 – February 2019, inclusive). All indicators show that retrieval
328 sensitivity is greater over land than water in the lower troposphere (“LT”; represented by the surface, 900
329 hPa and 800 hPa profile levels), with sharp differences evident at almost all land-water boundaries. The
330 sensitivity contrast clearly decreases in strength with height. By mid-tropospheric levels (“MT”; represented
331 by 600 hPa profile level), AK diagonal values and rowsums reach greater values on average over water than
332 land. Some strong land-water gradients remain present in VMR ret-apr fields, most notably over North
333 Africa, the Arabian peninsula, and south-east China, but on average these values are much more similar
334 across land and water than in the LT. No clear land-water contrast is evident in the upper troposphere (“UT”;
335 represented by the 300 hPa profile level), with retrieval sensitivity instead varying more with latitude,
336 decreasing towards both poles (a companion to Fig. 3 with an altered colour bar to better show spatial patterns
337 in AK diagonal values and rowsums at MT and UT levels is provided in the Supp. Mat. (SM1)).

338 AK diagonal values and rowsums show that retrieval sensitivity increases across both land and water
339 with height. It is lowest at the surface level, with little information content in the retrieval over water (AK

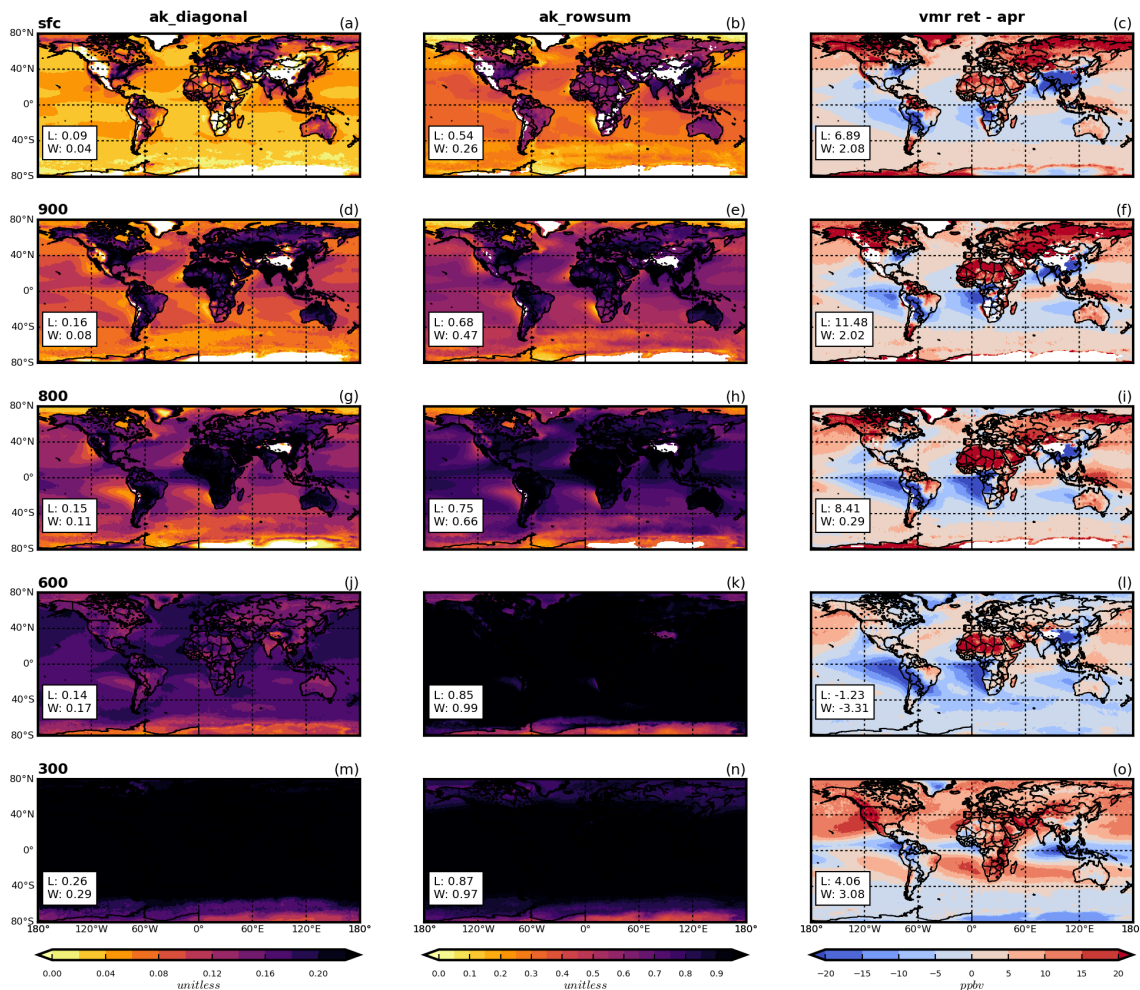


Figure 3. Mean sensitivity metrics from MOPITT L3 data, averaged across the entire study period (September 2001 – February 2019, inclusive). Shown are AK diagonal values (left column), AK rowsums (center column) and VMR retrieved minus a priori values (right column) for the following levels of the retrieved profile: surface (top row), 900 hPa (second row), 800 hPa (third row), 600 hPa (fourth row), and 300 hPa (bottom row). Values in white boxes correspond to mean values across all land (“L”) and water (“W”) L3 grid boxes.

340

341 diagonal values and rowsums over water are less than half what they are over land, on average). There is high
 342 spatial variability over land: AK diagonal values and rowsums reach values comparable to those at higher
 343 profile levels in some sensitivity hotspots (e.g. parts of central Europe, east Asia, eastern USA and tropical
 344 west Africa), while being more comparable to values over water in other areas. By 800 hPa, AK diagonals



345 and rowsums over water reach values comparable to or greater than those reached over land at the surface
346 level, in most places.

347 Spatial patterns in retrieved minus a priori VMRs are slightly more complex to interpret, because they
348 are influenced both by retrieval sensitivity and the accuracy of the a priori. For example, while values close
349 to zero can indicate a retrieval that is heavily weighted by the a priori and therefore low retrieval sensitivity,
350 they can also indicate that the true VMR is close to the a priori value. Despite this, retrieved minus a priori
351 VMR values clearly reach more strongly positive or negative values over land than water in the LT, with the
352 contrast becoming less pronounced with height. Furthermore, there are clear land-water change points in the
353 LT, especially in the LT. This further demonstrates the impact of the land-water contrast in retrieval
354 sensitivity.

355

356

357 **3.1.2. Analysis of coastal L3 grid boxes**

358

359 Scatterplots of sensitivity metrics at selected profile levels, for coastal L3 grid boxes only, are shown in Fig.
360 4. Specifically, these plots show the sensitivity of the L2 land and water retrievals that are bounded by the 1°
361 x 1° L3 grid boxes and used to create the L3O data. The values that are plotted correspond to the long-term
362 mean from the L3L and L3W datasets for these grid boxes. For this comparison, the L3L and L3W means
363 are only calculated from days when L2 retrievals over both land and water are present and the L3O surface
364 index is mixed. This minimises potential differences in the true CO profiles that could arise due to temporal
365 variations for the L3L and L3W pairings being compared. Furthermore, it allows for the analysis of the
366 resulting L3O_M data on these days with knowledge of the parent L2 retrievals over land and water and their
367 differences. For ease of interpretation, the absolute retrieved minus a priori VMR values are plotted, i.e.
368 ignoring whether the result is positive or negative. However, the results hold if using signed values, and a
369 duplicate of Fig. 4 with signed retrieved minus a priori VMR values is included in the Supp. Mat. for reference
370 (SM2).

371 The AK diagonal value and rowsum plots clearly demonstrate greater sensitivity over land (L3L) than
372 over water (L3W) at LT levels (a point below the diagonal line on these panels indicates greater values in
373 L3L) for the majority of grid boxes, with the difference decreasing into the MT and UT. Correspondingly,
374 retrieved VMRs also deviate more greatly from their a priori values in L3L than L3W in the LT, with smaller
375 land-water differences in the MT and UT. Mean values are significantly different ($p < 0.005$) apart from AK
376 diagonal values and retrieved minus a priori VMR at 300 hPa ($p = 0.13$ and 0.07 respectively). Sensitivity
377 metrics are generally better correlated in the MT and UT than at LT levels.

378

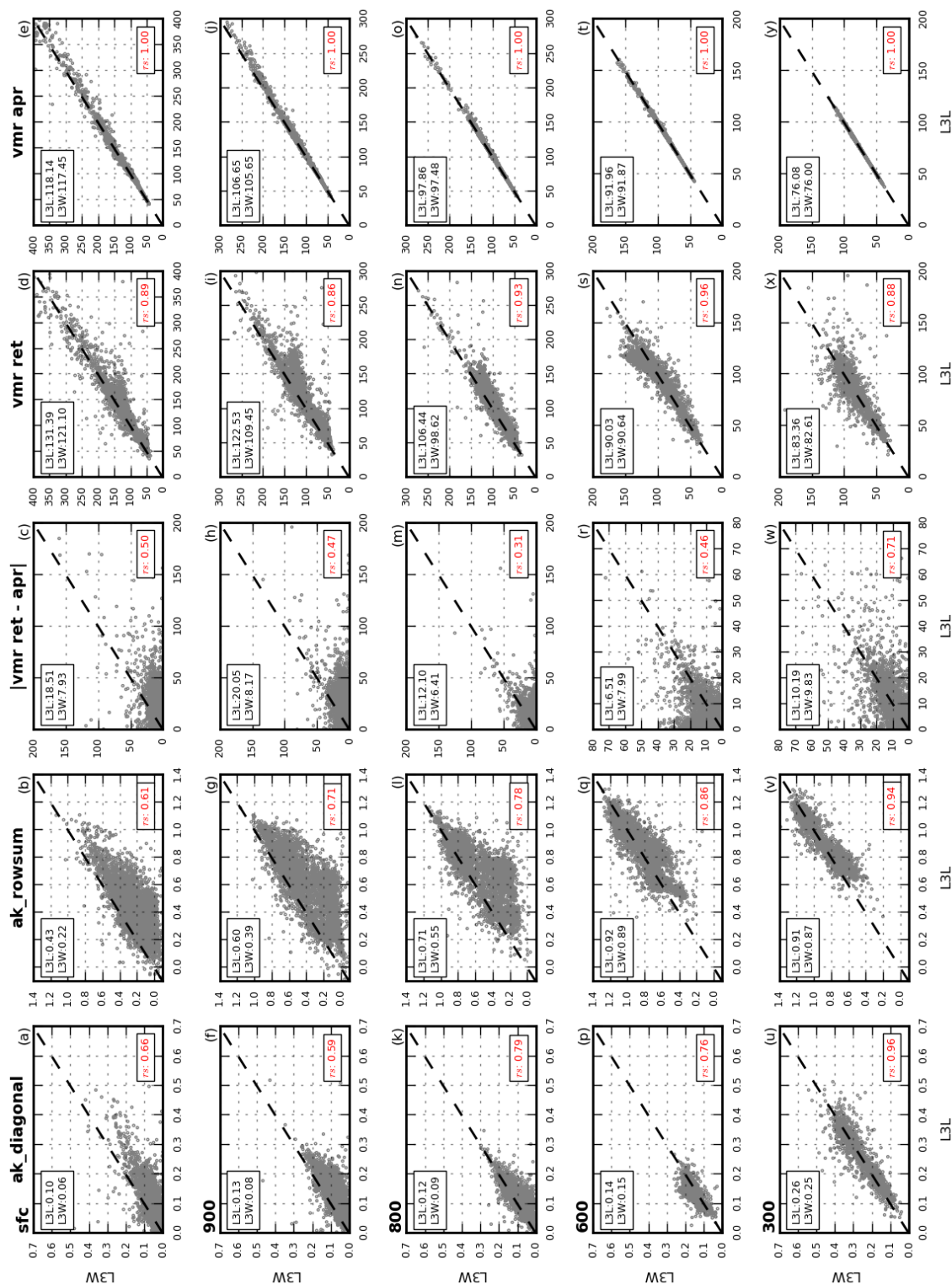




Figure 4. Mean sensitivity metrics and VMRs (retrieved and a priori) from coastal L3 grid boxes. Values compared in the scatterplots are mean values from matched L3L and L3W retrievals within these grid boxes. “Matched” means that only days when both L3L and L3W are present, and the L3O surface index is mixed, are used to create the mean values analysed. Shown are AK diagonal values (left column), AK rowsums (second column), absolute VMR retrieved minus a priori values (third column), retrieved (fourth column) and a priori (fifth column) VMRs, for the following levels of the retrieved profile: surface (top row), 900 hPa (second row), 800 hPa (third row), 600 hPa (fourth row), and 300 hPa (bottom row). Values in boxes in the top-left corner of each panel correspond to mean values across all L3L and L3W grid boxes. These means are significantly different using a 2-tailed t-test (unequal variance) with $p < 0.005$ in all cases except $ak_diagonal$ at 300 hPa where $p = 0.13$, $vmr_ret_minus_apr$ at 300 hPa where $p = 0.07$, vmr_ret at 600hPa where $p = 0.30$, vmr_ret at 300hPa where $p = 0.11$. No vmr_apr mean differences are significant. Values in the bottom-right corner of each panel correspond to the Spearman’s rank correlation coefficient ($p < 0.005$ in all cases).

379

380 This analysis clearly shows how L2 retrievals that are averaged together to create the L3O data over
381 coastal grid boxes on days when the surface index is mixed have differing degrees of sensitivity, especially
382 in the LT. This is explicitly cautioned against in the MOPITT data user’s guide (MOPITT Algorithm
383 Development Team, 2018). The remainder of this paper focuses on the surface-level of the retrieved profile,
384 since the LT is where discrepancies are greatest, and the cause of this sensitivity contrast is well established
385 (as outlined in the introduction).

386

387

388 **3.2. Differences in retrieved VMRs and temporal trends, and their relation to the land-water sensitivity** 389 **contrast**

390

391 **3.2.1. L3L vs L3W**

392

393 *Retrieved VMR comparison between L3L and L3W*

394

395 In addition to the clear land-water LT sensitivity contrast in coastal grid boxes, there are (sometimes large)
396 differences in the retrieved VMRs (Fig. 4; Fig. 5a (black boxplots)). The retrievals performed over land yield
397 surface-level VMRs that are over 10 ppbv greater than over water, on average. As with sensitivity, land-
398 water differences in retrieved VMRs decrease higher up in the profile. Although a decrease in VMRs from
399 land to water might be expected in the LT, given that most CO sources are land-based, the land-water
400 difference in LT retrieved VMRs is well over 10 times greater than in the a priori VMRs used for the retrievals
401 (also shown in Fig. 4; mean difference = 10.29 vs 0.69 ppbv, respectively, for surface level). Furthermore,



402 this assumption only seems reasonable where large CO sources are proximal to the coastline, as it is
403 unrealistic to expect such large gradients in background CO (which coastal grid boxes far from large CO
404 sources are more likely to represent) across a relatively small distance – as is verified by the a priori VMR
405 comparison which suggests the land-water difference in CO concentrations should be negligible for the
406 majority of the grid boxes compared.

407 Greater land-water sensitivity differences tend to be associated with greater retrieved VMR
408 differences. Figure 5b shows the distribution of retrieved surface level VMR differences (L3L – L3W)
409 stratified by the corresponding surface level AK rowsum difference. Larger retrieved VMR differences are
410 clearly associated with greater AK rowsum differences (some degree of spread in the results is expected,
411 since the relationship also depends on the accuracy of the a priori, as outlined previously). Absolute retrieved
412 VMR difference values are shown in Fig. 5b for clarity, since L3L – L3W can be either positive or negative
413 depending on whether a priori VMRs used in the retrieval are greater or less than the “true” VMR being
414 retrieved, which complicates the analysis. The corresponding plot with raw values (i.e. not discarding the +/-
415 sign) is included in the Supp. Mat. however, and the same conclusions can be drawn based on this figure
416 (SM3).

417 Of the 3971 coastal grid boxes that are compared, 60 % (2379) show a significant difference ($p < 0.1$,
418 determined using a 2-tailed student’s t-test) in mean VMRs in L3L and L3W (Fig. 5a). Compared to grid
419 boxes where the mean VMR difference is not significant, there are several notable differences (detailed in
420 Table 1). As expected from the previous analysis, the land-water sensitivity contrast is greater when mean
421 VMRs are significantly different than when not. This is evident in AK rowsum and VMR retrieved minus a
422 priori differences (the magnitude of difference between significance subsets is around 50 % and 100 %,
423 respectively). Interestingly, the AK difference is due to sensitivity being lower over water when VMRs are
424 significantly different than when they are not; sensitivity over land is similar in both subsets. This may be
425 explained as follows: when sensitivity over water is especially low, as is the case in the significant-difference
426 subset, the retrieved VMR will be heavily weighted by the a priori and unable to match the variation present
427 in the more sensitive retrieval over land. As sensitivity over water increases, this a priori weighting weakens
428 and the retrieved VMR will more closely track the retrieval over land, resulting in a less significant difference.
429 Also of note, a priori VMRs are much lower when retrieved VMRs are significantly different than when they
430 are not, on average. Considered alongside the greater retrieved minus a priori differences, this suggests that
431 the a priori VMR could be a less accurate estimate of the “true” VMR for the significant-difference subset,
432 whereas it is closer to reality when retrieved VMRs over land and water are not significantly different.
433 Intuitively, this makes sense: for a hypothetical situation where the a priori VMR is a perfect match for the
434 “true” VMR, and both are uniform across a coastal L3 grid box, retrievals over the land and water grid box

435

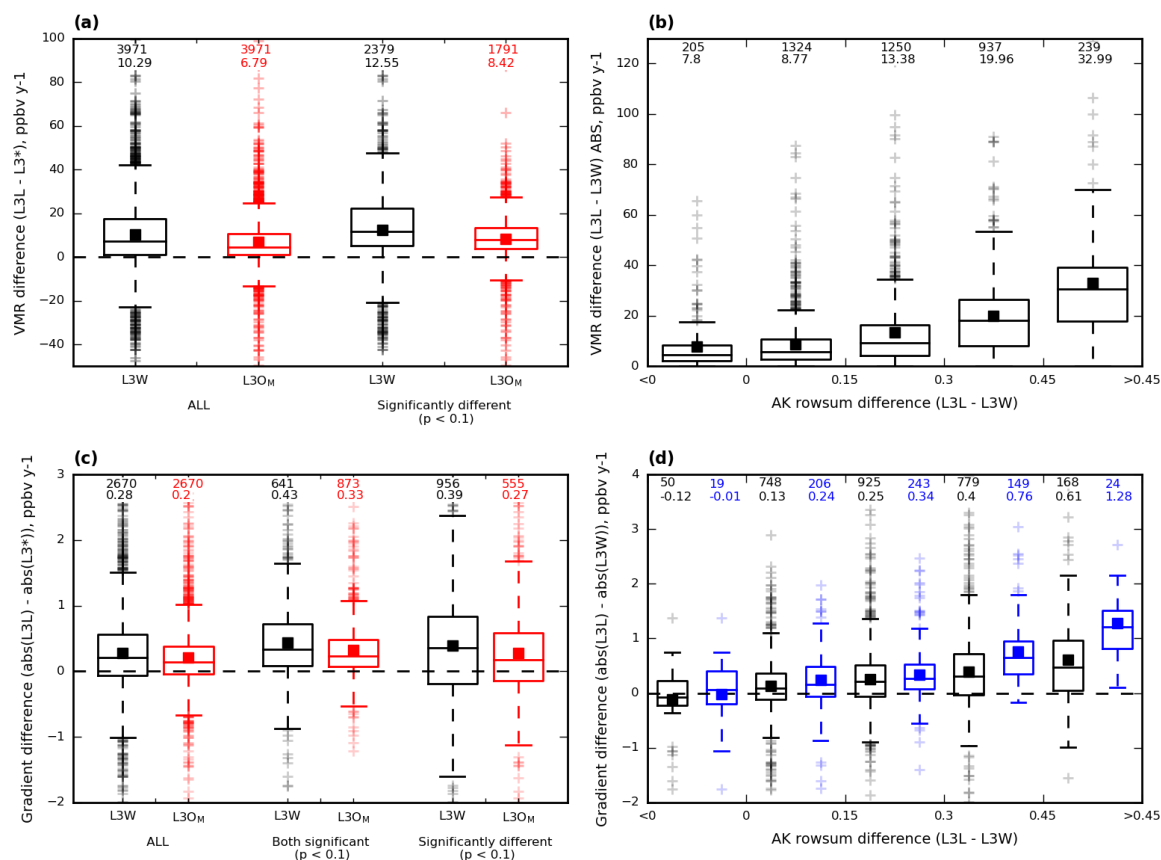


Figure 5. Boxplots showing how mean VMRs and trends from WLS analysis compare for coastal L3 grid boxes, calculated from matched retrievals within these grid boxes. “Matched” means that only days when both L3L and L3W are present and the L3O surface index are mixed are used to create the mean values analysed. Mean values are represented by filled squares, and values above the boxplots correspond to number of grid boxes with data for that boxplot, and the mean value, respectively. **(a)** Mean VMR differences for L3W (black) and L3O_M (red) compared to L3L (L3L – L3* in both cases). Shown are the differences for all coastal grid boxes, and only for those grid boxes where the difference is significant ($p < 0.1$), determined using a 2-tailed t-test. **(b)** Absolute mean VMR differences between L3L and L3W, stratified according to corresponding AK rowsum difference (L3L – L3W in both cases). **(c)** Absolute differences in gradients detected using WLS regression analysis for L3W (black) and L3O_M (red), compared to L3L (L3L – L3* in both cases). Shown are differences for all coastal grid boxes where WLS analysis could be performed, for grid boxes where both trends compared are significantly different to zero ($p < 0.1$), and for grid boxes where the trend difference is significant ($p < 0.1$). **(d)** Absolute differences in gradients detected using WLS regression analysis between L3L and L3W, stratified according to corresponding AK rowsum difference (L3L – L3W in both cases). Shown are the differences for all coastal grid boxes where WLS could be performed (black), and only for those grid boxes where the detected trend is significant ($p < 0.1$) in both L3L and L3W (blue).



436

Table 1. Mean values for selected variables from L3L and L3W for coastal L3 grid boxes, matched retrievals only. “Matched” means that only days when both L3L and L3W are present and the L3O surface index are mixed are used to create the mean values analysed. Mean values are calculated and presented separately according to the results of a 2-tailed student’s t-test (unequal variance) performed on mean retrieved VMR values in L3L and L3W (n = 3971).

	P < 0.1 (n=2379, 60 %)			P > 0.1 (n=1592, 40 %)		
	land	water	d	land	water	d
Mean vmr_ret	129.97	117.41	12.55	133.52	126.60	6.90
Mean vmr apr	113.78	113.18	0.61	124.65	123.83	0.83
Mean ret-apr	16.18	4.24	11.94	8.87	2.77	6.09
Mean ak rowsum	0.43	0.18	0.24	0.44	0.27	0.16

437 subsets would be expected to be identical irrespective of any differences in retrieval sensitivity over those
438 surfaces. To summarise: assuming “true” VMRs are similar over land and water within coastal L3 grid boxes,
439 differences in retrieved VMRs depend not only the sensitivity of the retrieval, but also on the accuracy of a
440 priori VMRs used in the retrievals.

441

442 *Trend comparison between L3L and L3W*

443

444 Temporal trends detected in L3L and L3W are now compared. The aim here is to demonstrate that there are
445 trend differences between L3L and L3W datasets for coastal gridboxes that can be related to AK differences.
446 An underlying assumption is that the temporal trend in “true” VMRs should not vary much across a 1° x 1°
447 L3 grid box. Hedelius et al. (2021) lends credence to this assumption with the finding that CO trends are
448 similar within regions spanning a few thousand kilometres (L3 grid boxes are ~ 100 km²), and that trends
449 within urban areas are generally indistinguishable from the trend of the broader region encompassing the
450 urban area, despite an assumption that urban trends should exceed the regional background due to a
451 concentration of CO emissions here. Gradients obtained from WLS regression on each dataset are compared,
452 subtracting the trend in L3W from the trend in L3L. For clarity, differences between the absolute trend values
453 (i.e. ignoring the +/- sign of the trend) are presented, since this shows the degree of difference in the trend
454 magnitude, irrespective of trend direction. A positive trend difference in this case signifies a stronger (faster)
455 trend in L3L than L3W.



456

Table 2. Descriptive stats corresponding to the WLS trends detected in L3L, L3W, and L3O_M that are compared in the boxplots of Fig. 5c.

			Mean	Std	Median	IQR
All	L3L – L3W (n = 2670)	L3L	-0.55	1.27	-0.47	1.00
		L3W	-0.49	1.08	-0.34	0.65
	L3L – L3O _M (n = 2670)	L3L	-0.55	1.27	-0.47	1.00
		L3O _M	-0.51	1.03	-0.38	0.73
Both significant (p < 0.1)	L3L – L3W (n = 641)	L3L	-1.39	1.66	-1.15	1.08
		L3W	-1.06	1.56	-0.78	0.92
	L3L – L3O _M (n = 873)	L3L	-1.24	1.64	-1.06	1.07
		L3O _M	-1.02	1.38	-0.83	0.88
Significantly different (p < 0.1)	L3L – L3W (n = 956)	L3L	-0.64	1.39	-0.65	0.92
		L3W	-0.52	1.06	-0.43	0.67
	L3L – L3O _M (n = 555)	L3L	-0.69	1.36	-0.67	0.85
		L3O _M	-0.60	1.00	-0.51	0.68

457 On average, across all grid boxes where WLS can be performed in both datasets following the criteria
 458 outlined in Sect. 2.5 (n = 2670), trends are stronger in L3L than L3W (Fig. 5c (black boxplots)), with the
 459 range of differences around 2.5 ppbv y⁻¹ (~-1 ppbv y⁻¹ to 1.5 ppbv y⁻¹). When the comparison is restricted to
 460 grid boxes where both trends are significantly different to zero (p < 0.1; 641 of the 2670 grid boxes, 24 %),
 461 a greater proportion of those grid boxes have a stronger trend in L3L than L3W (> 75%), but the overall
 462 range of differences doesn't shift by much. The L3L – L3W trend difference is significant in 956 of the 2670
 463 coastal grid boxes for which the analysis can be performed (36 %), with the range in differences spanning
 464 around 4 ppbv y⁻¹. Analysis of the distribution of differences between the raw trend values (i.e. including the
 465 +/- sign) is complicated because negative differences can have multiple meanings. However, trends are
 466 negative at 75 % of coastal grid boxes in both datasets (this increases to 95% when the trend in both L3L and
 467 L3W is significant), with retrieved surface CO concentrations over land decreasing at a faster rate than over
 468 water, on average (descriptive stats associated with raw trend values are detailed in Table 2).

469 To determine whether differences in trend can be linked to differences in retrieval sensitivity, L3L –
 470 L3W trend differences (again, based on absolute WLS trend values) are stratified by L3L – L3W surface
 471 level AK rowsum differences (Fig. 5d). As with mean VMR differences, the size of the trend difference tends
 472 to increase as the difference in AK rowsums increases. In addition, as the magnitude of rowsum difference
 473 increases in the positive direction (i.e. increasingly greater sensitivity over land), a greater proportion of trend



474 differences are positive (i.e. a stronger trend over land). This pattern is even more pronounced when restricted
475 to grid boxes where both trends are significant (also shown in Fig. 5d).

476 All together, these results show that within coastal L3 grid boxes, differences in retrieval sensitivity
477 over land and water are related to differences in temporal trends identifiable in corresponding surface-level
478 retrievals. The relationships found in these analyses are not perfect because trend differences are sensitive to
479 several other factors, in addition to differences in retrieval sensitivity. For example, a greater trend difference
480 would be evident if the rate of change in “true” CO concentrations is faster than if it is slow/negligible, for a
481 given sensitivity difference. Similarly, there should be zero trend difference if “true” CO concentration levels
482 are stable over time, irrespective of the magnitude of difference in retrieval sensitivity. The accuracy of the
483 a priori is a further complicating factor. However, the results presented do imply a general tendency for trend
484 underestimation in retrievals over water within coastal grid boxes compared to retrievals over land in the
485 same grid boxes obtained at the same times, which appears to be linked to differences in retrieval sensitivity.

486

487

488 3.2.2. Consequences for L3O_{Mixed}

489

490 To recap, L3O data are given the surface index “mixed” when neither land nor water is the dominant surface
491 type of the bounded L2 retrievals, for a given retrieval time. When this is the case, the retrievals over land
492 and water are averaged together. Users of L3O data do not have the option of choosing to only analyse the
493 subset of retrievals made over land (L3L) or water (L3W), as was done in the preceding analysis. To do so
494 requires the original L2 retrievals. In this section, the L3O_M retrievals are compared to the L3L retrievals that
495 were analysed in the previous section. The aim here is to demonstrate how, for some L3 grid boxes,
496 information on “true” VMRs and temporal trends that is available in the L2 retrievals over land (L3L) is
497 effectively lost to users of L3O data by their averaging together with the less sensitive L2 retrievals over
498 water (L3W).

499

500 *Retrieved VMRs in L3O_M*

501

502 For long-term mean VMRs, L3O_M unsurprisingly represents a mid-point between L3L and L3W, with lower
503 VMRs and weaker trends than L3L, but a smaller difference range overall than L3W (Fig. 5a). The L3L –
504 L3O_M differences in long-term mean VMR are significant at 45 % (1791) of coastal grid boxes. All but 3 of
505 these also see a significant difference between long-term mean VMRs in L3L and L3W. This makes sense:
506 retrievals in L3L would not be expected to differ significantly from those in L3O_M if they do not also differ



507 significantly from L3W. In total, 75 % of grid boxes that feature a significant difference between L3L and
508 L3W also see a corresponding significant difference between L3L and L3O_M. There are several notable
509 differences between this subset of coastal grid boxes (“BOTH”), compared to those that see a significant
510 difference between L3L – L3W but not between L3L and L3O_M (“L3L_L3W_ONLY”; detailed in Table 3a):

511

- 512 • The grid boxes of BOTH see greater retrieved VMR differences between L3L and L3W than the grid
513 box subset of L3L_L3W_ONLY (mean L3L – L3W difference of 13.84 vs 8.67 ppbv). This is logical:
514 L3O_M only differs significantly from L3L if the underlying L3L – L3W difference is sufficiently large
515 to persist through the averaging.
- 516 • The grid boxes of BOTH also feature a greater land-water sensitivity contrast than those of
517 L3L_L3W_ONLY. This is indicated both by L3L – L3W AK rowsum differences, driven
518 predominantly by decreased sensitivity over water in BOTH; and by L3L – L3W retrieved minus a
519 priori VMR differences.
- 520 • The grid boxes of BOTH tend to have a greater proportion of their surface covered by water than
521 land. This is quantified by comparing the mean number of L2 retrievals over land and water that are
522 averaged together to make L3L and L3W each day (“n_ret(L3L)” and “n_ret(L3W)”), for each coastal
523 grid box compared. A mean n_ret(L3L/L3W) ratio of 0.87 for BOTH indicates a greater water
524 influence on L3O_M than for the grid boxes of L3L_L3W_ONLY, for which a mean n_ret(L3L/L3W)
525 ratio of 1.00 indicates a more even land/water split. Thus, L3O_M more closely resembles L3W – which
526 is significantly different to L3L – in BOTH than in L3L_L3W_ONLY.

527

528 It is easy to understand how each of these can lead to a L3O_M retrieval that differs significantly from
529 the corresponding L3L retrieval. In addition to the differences between the grid boxes of BOTH and
530 L3L_L3W_ONLY outlined above, it is also notable that retrieved and a priori VMRs are lower in BOTH
531 than in L3L_L3W_ONLY, and that retrieved minus a priori VMR values are greater in BOTH than in
532 L3L_L3W_ONLY. This could imply that the a priori VMRs are closer to reality for the grid boxes of
533 L3L_L3W_ONLY than those of BOTH, however further information on “true” VMRs is required to properly
534 assess this.

535

536 *Trends in L3O_M*

537

538 Temporal trends detected in L3O_M are now compared to those in L3L. Overall, a greater number of grid
539 boxes feature a significant trend in both L3L and L3O_M than in L3L and L3W (873 vs 641; 33 % vs 24 %),



540

Table 3a. Descriptive stats corresponding to matched retrievals over land and water (L3L and L3W) where the long-term mean retrieved surface level VMR in L3L and L3W is significantly different ($p < 0.1$, $n = 2379$). Grid boxes are divided into two subsets depending on whether long-term mean VMRs in L3L and L3O_M are significantly different ($p < 0.1$; “BOTH”) or not ($p > 0.1$; “L3L_L3W_ONLY”). $n_{\text{ret}}(\text{L3L})$ ($n_{\text{ret}}(\text{L3W})$) = the number of L2 retrievals over land (water) used to make a retrieval in L3O_M. A ratio $n_{\text{ret}}(\text{L3L}/\text{L3W})$ value > 1 (< 1) implies that more of the L3 grid box surface is covered by land (water).

	BOTH ($n = 1788$, 75 %)			L3L_L3W_ONLY ($n = 591$, 25 %)		
Mean $n_{\text{ret}}(\text{L3L}/\text{L3W})$	0.87			1.00		
	Land	Water	L-W	Land	Water	L-W
Mean vmr_ret	127.21	113.37	13.84	138.30	129.64	8.67
Mean vmr_apr	109.11	108.62	0.49	127.94	126.96	0.98
Mean ret_apr	18.11	4.75	13.36	10.36	2.68	7.68
Mean AK rowsum	0.42	0.16	0.26	0.46	0.26	0.20

Table 3b. Descriptive stats corresponding to matched retrievals over land and water (L3L and L3W) where the temporal trend detected using WLS regression analysis on yearly-mean retrieved surface level VMR in L3L and L3W is significantly different ($p < 0.1$, $n = 956$). Grid boxes are divided into two subsets depending on whether the trend in L3L is significantly different to the corresponding trend detected in L3O_M ($p < 0.1$; “BOTH”) or not ($p > 0.1$; “L3L_L3W_ONLY”). $n_{\text{ret}}(\text{L3L})$ ($n_{\text{ret}}(\text{L3W})$) = the number of L2 retrievals over land (water) used to make a retrieval in L3O_M. A ratio $n_{\text{ret}}(\text{L3L}/\text{L3W})$ value > 1 (< 1) implies that more of the L3 grid box surface is covered by land (water).

	BOTH ($n = 447$, 47 %)			L3L_L3W_ONLY ($n = 509$, 53 %)		
Mean $n_{\text{ret}}(\text{L3L}/\text{L3W})$	0.77			0.99		
	Land	Water	L-W	Land	Water	L-W
Mean WLS trend	-0.72	-0.58	-0.14	-0.58	-0.47	-0.11
Mean ABS WLS trend	1.18	0.76	0.42	1.04	0.68	0.35
Mean trend standard error	0.55	0.39	0.16	0.58	0.36	0.22
Mean vmr_ret	128.25	121.36	6.90	129.22	120.20	9.02
Mean vmr_apr	117.21	117.13	0.08	116.01	115.73	0.29
Mean ret_apr	11.05	4.22	6.82	13.21	4.47	8.74
Mean AK rowsum	0.46	0.22	0.25	0.44	0.20	0.24



541 and fewer see a significant difference between trends (555 vs 956; 21 % vs 36 %). The trends in L3L and
542 L3O_M are significantly different in just under half (47 %) of the grid boxes where the trend is also significantly
543 different between L3L and L3W (“BOTH”; Table 3b). The ratio $n_{\text{ret}}(\text{L3L}/\text{L3W})$ clearly shows that these
544 grid boxes are more water-dominated (mean ratio = 0.77) than the remaining 53 % grid boxes that feature a
545 significant difference between trends in L3L and L3W but not L3O_M (“L3L_L3W_ONLY”; mean ratio =
546 0.99). Additionally, detected trends in the grid boxes of BOTH are slightly stronger, with a greater difference
547 between L3L and L3W, than for the L3L_L3W_ONLY subset. Those L3 grid boxes featuring the strongest
548 land-water trend difference are therefore most likely to also see a significant trend difference between L3L
549 and L3O_M. Again, this is logical. Unlike with the retrieved VMR comparison above, there are no clear
550 differences in mean retrieved or a priori VMRs, nor sensitivity metrics, between these two grid box subsets
551 (also detailed in Table 3b). However, it is not necessarily expected that there would be clear differences in
552 these parameters for this analysis, since trend magnitudes themselves are a variable.

553 Most of the grid boxes where the L3L and L3O_M trends are significantly different also feature a
554 significant difference between L3L and L3W (453 of 555; 82 %). There are no clear differences between
555 these and the remaining 18 % of grid boxes that, counter-intuitively, feature a significant difference between
556 trends in L3L and L3O_M but not between trends in L3L and L3W. However, small discrepancies are to be
557 expected for results based on statistical thresholds, especially where the variables being compared are subject
558 to multiple different factors (e.g. land-water surface cover ratio in L3O_M; land-water sensitivity contrast;
559 retrieved VMR differences; differences in the “true” CO concentration being retrieved and its change over
560 time).

561

562

563 3.3. Implications for users of L3O data

564

565 So far, this paper has shown a clear difference in retrievals over land and water for coastal grid boxes,
566 demonstrated how results using these retrievals (L3L and L3W) differ, and outlined consequences (in terms
567 of long-term VMR statistics and temporal trends) of averaging these retrievals together to create L3O_M. The
568 full timeseries of available data in L3O is now compared with L3L and L3W, without the constraint that a
569 retrieval needs to be present in both L3L and L3W for it to be included in the analysis. This replicates what
570 a user of the L3O data would do, i.e., work with all available data.

571 Users of MOPITT data are advised to restrict their analysis to retrievals performed over land. This
572 poses a quandary for users of L3O: what to do about days with a surface index of mixed? Therefore, the
573 implications of choosing to include or discard these days are also considered. In the subsequent sections, the



574 following subsets of the full L3O timeseries for each coastal gridbox are analysed: the full L3O timeseries
575 with no filtering by surface index (“L3O_{NF}”); only days with a surface index of land (“L3O_L”); and days
576 where the surface index is land or mixed (“L3O_{LM}” – i.e., only days with a L3O surface index of water are
577 discarded).

578

579

580 3.3.1. Loss of available data

581

582 This section analyses how L3L and the L3O subsets compare in terms of the overall number of days with
583 retrievals available for analysis at coastal grid boxes (total coastal grid boxes = 4299). To begin with, these
584 are compared to the total number of days available for analysis in L3O_{NF} (“n_days(L3O_{NF})”; Fig. 6a). Most
585 strikingly, 67 % of coastal grid boxes see an L3O surface classification of land less than 5% of the time
586 (yielding a n_days(L3O_L/L3O_{NF}) ratio of 0.05 or less). Just less than half of these (35 % of the 4299 total
587 coastal grid boxes) have zero days classified as land in the L3O dataset (note that as a result of how coastal
588 grid boxes are classified (outlined in Sect. 2.3), all n_days(L3O_L/L3O_{NF}) ratios are below 0.5 (i.e. at best,
589 L3O has a surface classification of land on 50% of days)). The guideline to only analyse retrievals performed
590 over land thus results in a huge loss of data for coastal grid boxes when using the L3O dataset. Importantly,
591 retrievals over land are made on a large proportion of these filtered days; but they are either discarded
592 altogether, or averaged together with retrievals made over water. This point is demonstrated by comparison
593 to the n_days(L3L/L3O_{NF}) ratio. In contrast to a mean (median) n_days(L3O_L/L3O_{NF}) ratio of 0.08 (0.01), a
594 mean (median) n_days(L3L/L3O_{NF}) ratio of 0.44 (0.40) demonstrates the stark loss of data, something which
595 is further highlighted by the fact that well over half (56%) of coastal grid boxes see a n_days(L3L/L3O_L)
596 ratio > 25 (Fig. 6b), indicating that these L3 grid boxes have at least 25 times more days with retrievals made
597 over land than are available for analysis in the L3O dataset, if filtering guidelines are followed.

598 The situation can be improved for L3O users by keeping days when the L3O surface index is classified
599 as mixed, in addition to land (“L3O_{LM}”). Even in this best-case scenario however, L3O_{LM} sees less days with
600 data than L3L for 61% of coastal grid boxes (the ratio n_days(L3L/L3O_{LM}) is > 1 for 61 % of coastal grid
601 boxes; Fig. 6b). Moreover, the large proportion of these L3O_{LM} days where the surface index is mixed suffer
602 from the averaging together of retrievals over land with retrievals over water which, as has been shown, can
603 significantly impact the results of analyses using these data. This point is returned to in following sections.

604 Intuitively, it is to be expected that the ratio n_days(L3L/L3O_{LM}) should *never* be < 1. L2 retrievals
605 over land obviously contribute to days when L3O is classified as land, and should, by definition, also
606 contribute to days when L3O is classified as mixed. In these cases, L3L will therefore also be present.



607 However, there are two instances where L2 retrievals over land in fact do not contribute to a L3O retrieval
 608 classified as mixed. Firstly, L2 retrievals themselves also have a classification of mixed, when the L2 retrieval
 609 does not predominantly overlie water or land. L3O can thus have a surface classification of mixed when
 610 created from bounded L2 retrievals that are either only retrieved over a mixed surface, or a combination of
 611 mixed and water: in both cases, there are no L2 retrievals over land, and therefore no L3L. Secondly, analyses
 612 performed for this paper identified numerous instances where L3O is classified as mixed, but the only
 613 contributing L2 retrievals are retrievals over water. In these instances, L3O would therefore seem to be
 614 misclassified. On days when this is the case, there will be no corresponding L3L retrieval. This is documented
 615 further in the Supp. Mat. (SM4). Attempting to quantify the extent of this misclassification influence is
 616 beyond the scope of this paper. In the vast majority of cases where a given gridbox has a $n_days(L3L/L3O_{LM})$
 617 ratio < 1 , the difference is negligible (i.e. 75 % of these grid boxes have a ratio between 0.9 and 1).
 618 Irrespective, in terms of the number of days with retrievals available for analysis, L3L is an improvement
 619 over $L3O_{LM}$ for more grid boxes than it is not.
 620
 621

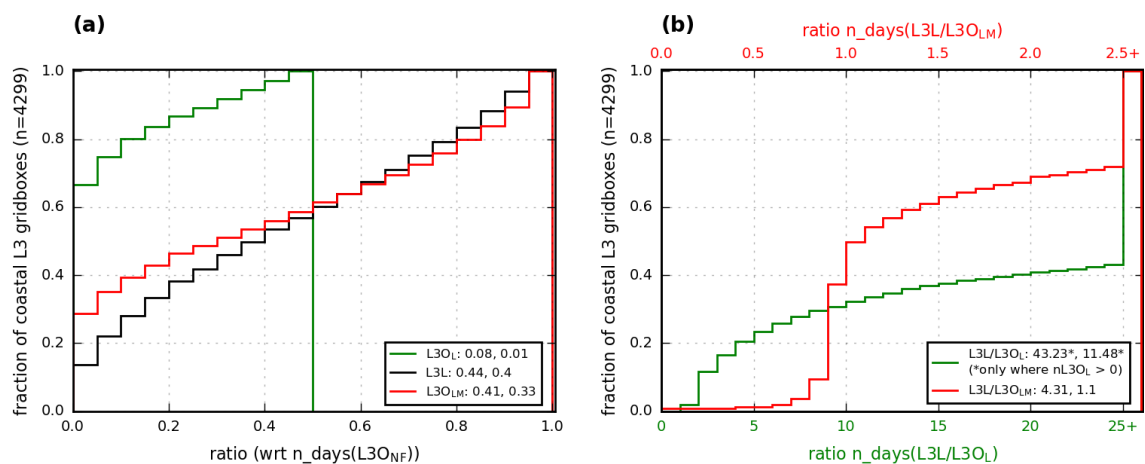


Figure 6. Cumulative frequency histograms comparing the number of days with data for different L3O subsets and L3L at coastal L3 grid boxes. A ratio < 1 (> 1) indicates the plotted dataset has less (more) days with data than the comparison dataset, indicated on the x-axis. **(a)** L3O_L (Green), L3L (black), and L3O_{LM} (red) are compared to the “as-downloaded” L3O dataset, without any filtering by surface index (“L3O_{NF}”). Values in legend correspond to mean and median ratio for indicated dataset, respectively. **(b)** L3L is compared with L3O_L (green line, bottom x-axis) and L3O_{LM} (red line, top x-axis). Values in legend correspond to mean and median ratios, respectively.



622 3.3.2. Scientific implications

623

624 Here, long-term mean (ltm) retrieved VMR values from the different L3 subsets are compared to L3L for all
625 coastal grid boxes. As expected from the analyses in Sect. 3.2, all L3 subsets that have some influence from
626 L2 retrievals over water have a ltm retrieved VMR that is below that in L3L, on average (Fig. 7a; note that
627 the n value is different for each boxplot because not all L3 subsets are present at every coastal grid box, as
628 discussed in Sect. 3.3.1). Unsurprisingly, the closest match to L3L is L3O_L (mean difference -3.1 ppbv), with
629 the mean difference increasing for each L3O subset as the influence of retrievals over water increases (e.g.
630 L3O_{LM} differs less on average from L3L (mean difference = 5.2 ppbv) than L3O_{NF} (mean difference = 9.1
631 ppbv)).

632 Note that ltm retrieved VMRs in L3O_L and L3L are not a perfect match because L3O_L is only a subset
633 of L3L for each grid box considered in the analysis: L3L may be present on a day when L3O_L is not owing
634 to the way that the L3O data are created (i.e., classified based on the ratio of L2 retrievals over land and
635 water, with retrievals over land potentially being discarded if these are not the majority). Apart from L3O_L,
636 less than 25 % of the coastal grid boxes have a retrieved ltm VMR that is greater in an L3O subset than in
637 L3L. The range of ltm differences for each of these L3O subset comparisons to L3L exceeds 35 ppbv
638 (excluding outliers), with over 25 % of coastal grid boxes compared having ltm differences exceeding 9 ppbv
639 (as indicated by boxplot upper quartile values).

640 The percentage of coastal grid boxes that feature a significant difference between ltm retrieved VMRs
641 in L3L and each L3O subset (indicated in red above each boxplot) is high: strikingly, it is found that, for the
642 two subsets that L3O users could realistically choose to analyse if following data filtering guidelines, almost
643 a quarter (L3O_L) or almost half (L3O_{LM}) of coastal grid boxes see a significant difference to L3L.

644 The results of WLS regression analysis on yearly mean values from each dataset are now compared.
645 As expected from the earlier analysis, trends are strongest, on average, in L3L and L3O_L – this is especially
646 so when the comparison is restricted only to trends that are significantly different from zero ($p < 0.1$) (Table
647 4). These datasets also have the largest measures of spread, indicating their tendency to yield stronger trends
648 than the other L3O subsets (and L3W), and these measures lessen for each L3O subset as the influence of
649 retrievals over water increases (e.g. standard deviations and inter-quartile ranges are smaller for L3O_{NF} and
650 L3W than L3O_L). Concomitant with trends decreasing in strength as the influence of retrievals over water
651 increases in each L3O subset, overall retrieval sensitivity also decreases, as indicated by the mean averaging
652 kernel metrics shown in Table 4. Comparing the magnitude of trends at each coastal grid box, trends are
653 stronger in L3L for at least 75% of grid boxes for all comparison datasets apart from L3O_L (Fig. 7b). L3O_L
654 sees stronger trends than L3L on average, but the comparison of these two datasets needs to be interpreted

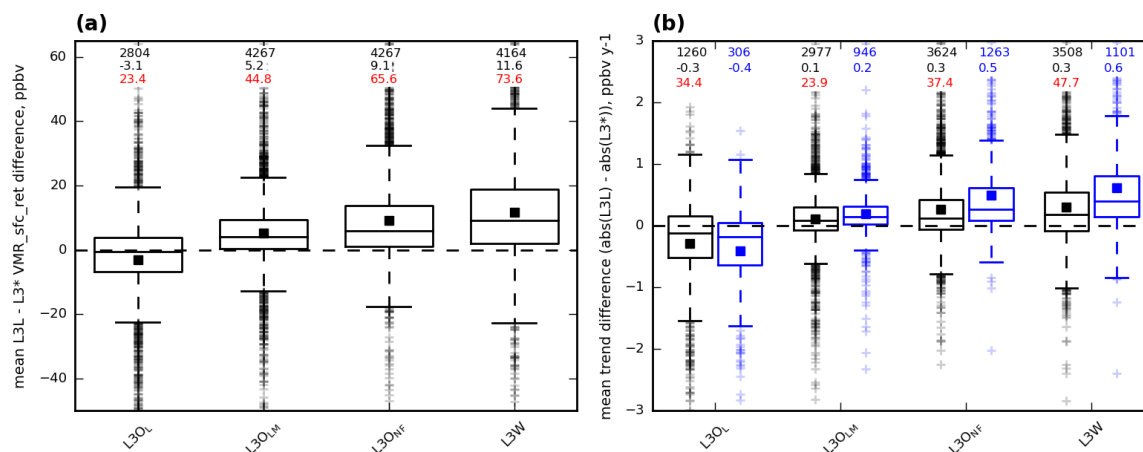


Figure 7. Boxplots showing how mean VMRs and trends compare from selected L3O subsets and L3W to L3L. Values compared are calculated from all available data across the study period. Mean values are represented by filled squares, and values above the boxplots correspond to number of grid boxes with data for that boxplot, the mean value, and the percentage of grid boxes represented in that boxplot that feature a significant difference with L3L (shown in red), respectively. The comparison is calculated as $L3L - L3^*$ in both cases; therefore a point above (below) the black $y=0$ line indicates that the value being compared is greater (lower) in L3L. **(a)** Mean VMR differences between L3L and the indicated L3O subset or L3W. **(b)** Differences in gradients (absolute values) detected using WLS regression analysis between L3L and the indicated L3O subset or L3W. Shown are the differences for all coastal grid boxes where WLS could be performed for both datasets compared (black), and only for the sample of those grid boxes where the detected trend is significant ($p < 0.1$) in both (blue).

Table 4. Descriptive stats corresponding to the WLS trends detected in L3L, L3W, and selected L3O subsets. Also shown are mean averaging kernel rowsums and diagonal values corresponding to the retrievals from which trends are calculated.

		L3L	L3O _L	L3O _{LM}	L3O _{NF}	L3W
Calculated from all gridboxes where WLS could be performed	Number of grid boxes	3624	1260	2999	4288	4169
	Mean (std) trend	-0.59 (1.22)	-0.52 (1.38)	-0.50 (0.95)	-0.54 (0.67)	-0.54 (0.66)
	Median (IQR) trend	-0.45 (0.89)	-0.46 (1.08)	-0.37 (0.67)	-0.42 (0.53)	-0.40 (0.54)
	Mean AK rowsum	0.45	0.45	0.33	0.28	0.22
	Mean AK diagonal value	0.10	0.10	0.08	0.07	0.06
Calculated only from gridboxes where WLS trend is significant ($p < 0.1$)	Number of grid boxes	1447	453	1265	2588	2499
	Mean (std) trend	-1.23 (1.55)	-1.17 (1.90)	-0.95 (1.18)	-0.79 (0.73)	-0.78 (0.72)
	Median (IQR) trend	-0.98 (0.94)	-1.09 (1.28)	-0.74 (0.75)	-0.62 (0.56)	-0.62 (0.57)
	Mean AK rowsum	0.51	0.48	0.39	0.33	0.29
	Mean AK diagonal value	0.11	0.10	0.08	0.07	0.06



656 with caution due to L3O_L being a subset of L3L that features far fewer days with data, as discussed previously.
657 Like with ltm retrieved VMRs discussed above, the percentage of coastal grid boxes that feature a significant
658 difference between trends detected in L3L and each L3O subset is high, with over a third (almost a quarter)
659 of the trends in L3O_L (L3O_{LM}) being significantly different to L3L.

660

661

662 3.4. Illustrative examples comparing L3O and L3L: analysis of the most populous coastal cities

663

664 Ltm VMRs and temporal trends from L3O_L and L3O_{LM} (the L3O subsets that data users would realistically
665 choose to analyse) are compared to those from L3L for the 33 coastal grid boxes that contain cities classified
666 amongst the 100 most populous in the world (derivation outlined in Sect. 2.5).

667

668 *VMR comparison:*

669

670 Mean VMRs calculated across the entire study period are shown in Fig. 8 for L3L, L3O_L, L3O_{LM}, and L3W
671 (included for comparison purposes). Comparing L3O_L to L3L, 6 of the 33 grid boxes analysed have no data
672 in the L3O_L subset. The mean $n_days(L3O_L/L3L)$ ratio for the remaining 27 cities is 0.19 (this raises slightly
673 to 0.23 if an additional 5 cities with only a few days (< 5) of data coverage are excluded). Only a single city
674 (Osaka) has more than 50 % of the L3L observation days in L3O_L. The consequence of this loss of data in
675 L3O_L is clear: mean VMR across all cities (excluding the 6 where $n_days(L3O_L) = 0$) is 17.2 ppbv higher
676 than in L3L (Table 5a). This falls to 9.8 ppbv if restricted to cities where the $n_days(L3O_L/L3L)$ ratio is
677 greater than 0.05 ($n=17$), and 6.8 ppbv if restricted to cities where the $n_days(L3O_L/L3L)$ ratio is above 0.2
678 ($n=11$). Mean VMR is significantly different ($p < 0.1$) for 11 of the 27 cities with $n_days(L3O_L) > 0$;
679 comparing these with the remaining cities that see no significant difference, cities with a significant
680 difference have a lower $n_days(L3O_L/L3L)$ ratio (i.e. relatively fewer retrieval days than L3L: ratio 0.15 vs
681 0.22), and much greater mean VMR differences (-36.49 vs -3.93 ppbv) (Table 5b).

682 L3O_{LM} compares more favourably to L3L in terms of number of observations, thanks to the inclusion
683 of days when the L3O surface index is “mixed”, with a mean $n_days(L3O_{LM}/L3L)$ ratio of 0.85.
684 $n_days(L3O_{LM}) > n_days(L3L)$ for 11 of the 33 cities, although the ratio is less than 1.05 (5 %) for all of
685 these except San Francisco and Istanbul (ratio = 1.14 and 1.35, respectively). The L3L – L3O_{LM} mean VMR
686 difference is relatively small (3.7 ppbv, all 33 cities; Table 5a). However, this does hide some much larger
687 discrepancies between L3L and L3O_{LM} for certain cities, with the difference exceeding 10 ppbv for 11 of the
688 33 cities and 20 ppb for 3 of them. The difference is significant ($p < 0.1$; “SIGDIFF”) for 13 of 33 cities (39

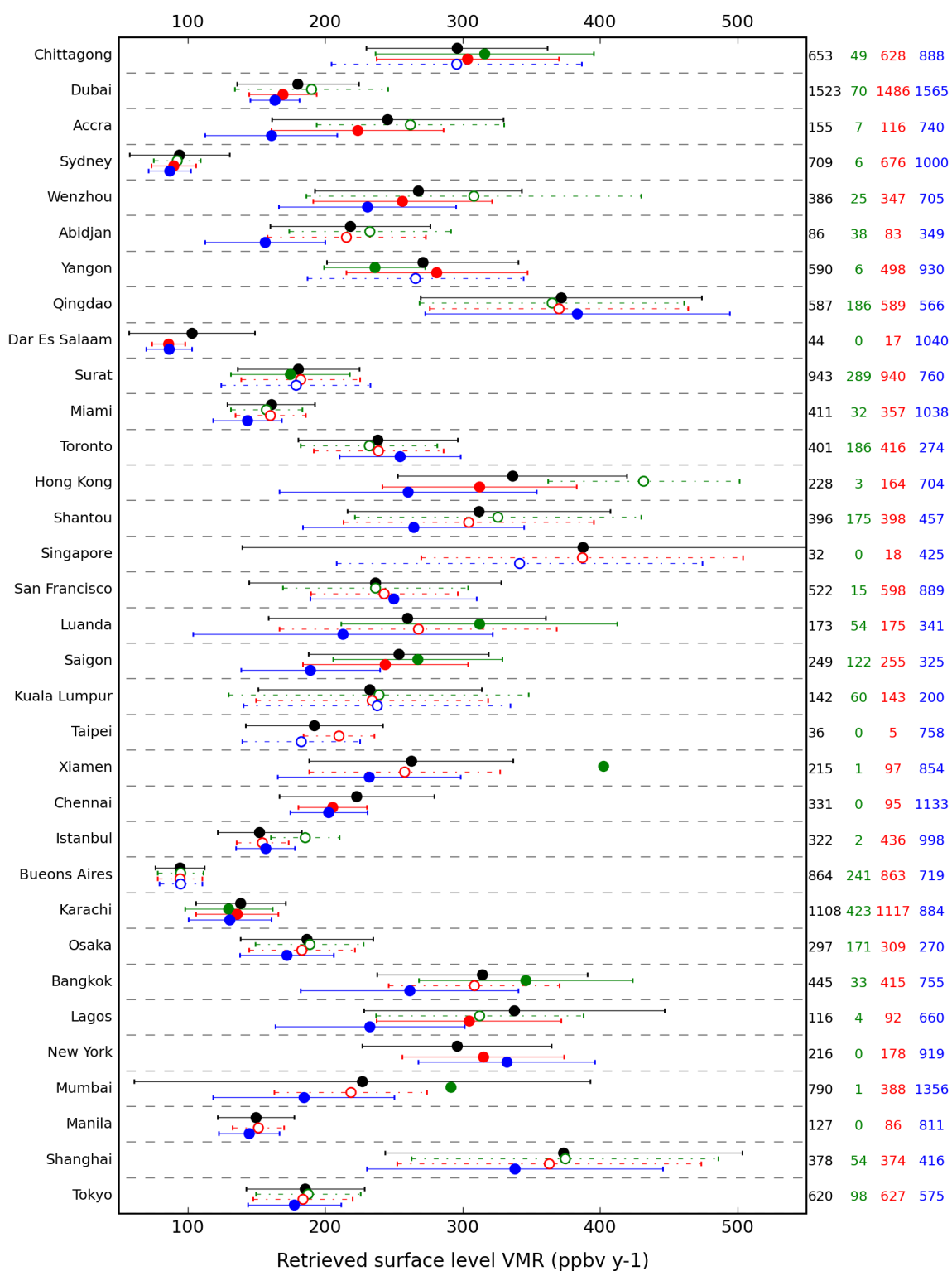




Figure 8. Comparison of long-term mean retrieved surface level VMR in L3L (black), L3O_L (green), L3O_{LM} (red), and L3W (blue), for the 33 largest coastal cities (ordered by population on the y-axis). The long-term mean value (in ppbv) is indicated by the filled/open circle on each row, and its standard deviation by the error bars. The L3L marker is always filled and lines are always solid. For other datasets, whether the marker is filled or not, and whether the lines are solid or dash/dot, depends on the outcome of an independent, 2-tailed t-test assuming unequal variance (aka “Welch’s test”) against L3L: filled markers and solid lines indicate the mean is significantly different to L3L ($p < 0.1$); open markers and dash/dot lines indicate there is no significant difference to L3L. The number of retrieval days in each time series analysed for each city is given on the right-hand y-axis, color-coded according to dataset.

Table 5. (a) Summary stats for mean VMRs across all cities analysed in Sect 3.4. “L3O_X” = L3O subset. **(b)** Selected parameters from L3 grid boxes containing cities where mean VMR in L3L and L3O_L is significantly different ($p < 0.1$). **(c)** Selected parameters from L3 grid boxes containing cities where mean VMR in L3L and L3O_{LM} is significantly different ($p < 0.1$).

(a)	L3L (n = 33)	L3O_L (n = 27)	L3O_{LM} (n = 33)	L3W (n = 33)
Mean (std) VMR_RET (ppbv)	235.6 (80.0)	255.2 (90.1)	231.9 (79.2)	212.2 (74.4)
Δ VMR_RET (L3L – L3O _X) (ppbv)	-	17.2	3.7	23.4
(b)	P < 0.1 (n = 11)	P > 0.1 (n = 16)		
ratio n_days(L3O _L /L3L)	0.15	0.22		
Δ VMR_RET (L3L – L3O _L) (ppbv)	-36.49	-3.93		
(c)	P < 0.1 (“SIGDIFF”) (n = 13)	P > 0.1 (“NOT_SIGDIFF”) (n = 20)		
ratio n_ret(L3L/L3W)*	0.51	1.02		
% days from L3O _L	9	20		
Δ VMR_RET (L3L – L3W) (ppbv)	31.15	18.44		
Δ AK rowsum (L3L – L3W)	0.25	0.21		
Δ AK diagonal (L3L – L3W)	0.10	0.08		
Δ VMR (RET - APR) (L3L – L3W) (ppbv)	21.66	3.22		
Δ VMR (RET - APR) (L3L – L3W) (ppbv)	21.98	11.88		
L3L VMR (RET - APR)	-19.82	-7.07		
L3L VMR (RET - APR)	39.86	18.79		
L3W VMR (RET - APR)	-14.75	-6.73		
L3W VMR (RET - APR)	18.21	15.57		

* n_ret(L3L) (n_ret(L3W)) = the mean number of L2 retrievals over land (water) that are averaged to make a L3L (L3W) retrieval



691 %). Compared to the subset where the L3L – L3O_{LM} mean difference is not significant (n = 20, 61 %;
692 “NOT_SIGDIFF”), the following characteristic differences are found (also detailed in Table 5c):

693

- 694 • The grid boxes are more water-dominated in SIGDIFF than NOT_SIGDIFF: this is evidenced by the
695 ratio of $n_{\text{ret}}(\text{L3L}/\text{L3W}) = 0.51$ vs 1.02 respectively; and also by the fact that on average, L3O_L only
696 contributes to SIGDIFF on 9 % of days, vs 20 % of days for NOT_SIGDIFF (which means that
697 retrievals over water contribute via L3O_M more frequently to SIGDIFF than NOT_SIGDIFF).
- 698 • The L3L – L3W VMR_RET differences are larger in SIGDIFF than NOT_SIGDIFF (mean = 31.15
699 vs 18.44 ppbv), meaning they are less likely to be hidden by averaging to create L3O_M.
- 700 • Although analysis of mean averaging kernels over land and water suggest there is not a large
701 sensitivity contrast between the SIGDIFF and NOT_SIGDIFF subsets (mean L3L – L3W rowsum
702 (diagonal value) differences are 0.25 vs 0.21 (0.10 vs 0.08) for SIGDIFF and NOT_SIGDIFF cities,
703 respectively), the L3L – L3W ret-apr difference, which is another indicator of sensitivity difference,
704 is much greater for SIGDIFF than NOT_SIGDIFF: 21.66 vs 3.22 ppbv respectively (21.98 vs 11.88
705 ppbv if using absolute values). There is some evidence that this may be a function of the a priori
706 values being closer to “true” VMRs in NOT_SIGDIFF: mean L3L retrieved minus a priori VMR
707 values fall from -19.82 ppbv for SIGDIFF to -7.07 ppbv for NOT_SIGDIFF (39.86 ppbv and 18.79
708 ppbv respectively, if using absolute values). A similar pattern is seen in L3W, although less
709 pronounced (-14.75 and -6.73 ppbv, respectively (18.21 and 15.57 ppbv if using absolute values)).

710

711 These findings are all consistent with what was shown in Sect. 3.2.2 when identifying factors that
712 determine whether the averaging of L2 retrievals over land and water to create L3O_M (the dominant
713 component of L3O_{LM} in all cases here, being the classification on 84 % of days, on average (max = 100 %,
714 min = 45 %)) can yield a statistically significantly different retrieval to L3L.

715

716 *Trend comparison:*

717

718 The above analysis is repeated with temporal trends detected using WLS regression. The trend values, their
719 associated standard errors, and an indication of their statistical significance ($p < 0.1$) are presented for each
720 city in Fig. 9. Where trend information is not plotted from a dataset for a given city, this means that there
721 were too few data points to perform the regression analysis.



722 On average, the strongest trends are seen in L3O_L. However, this often appears as an outlier compared
723 to the other datasets. As expected from previous sections, the weakest trends are detected in L3W, with
724 L3O_{LM} representing a mid-point between this and L3L.

725 Of the 18 cities where WLS analysis can be performed in L3O_L according to the criteria outlined in
726 Sect. 2.5, there are 9 cases where the trend is significantly different to that in L3L. In 3 of these cases (Dubai,
727 Wenzhou, Bangkok), despite being significant, the trend in L3O_L can be judged to be a huge over-estimate
728 given the trend comparison to L3L (standard errors do not overlap) and the very small number of days with
729 data compared to L3L ($n_{\text{days}}(\text{L3O}_L/\text{L3L})$ ratio < 0.08 in each case). There are 4 additional cities where a
730 significant trend in L3O_L appears to be an over-estimate on further analysis: Abidjan, Surat, Saigon, and
731 Buenos Aires. The trend for these cities in L3O_L is much stronger than in L3L (-1.6, -1.2, -2.2, and -0.4
732 ppbv/y, respectively), and the trend in L3L is also not significantly different to 0. Given the higher number
733 of days with data in L3L however ($n_{\text{days}}(\text{L3O}_L/\text{L3L})$ ratio = 0.44, 0.31, 0.49, 0.28, respectively), this
734 appears to be the more reliable result. The L3O_L trend for Miami is insignificant and derived from very low
735 n. L3O_L is also the only dataset to yield an insignificant trend for Qingdao.

736 As with mean VMRs, trends in L3O_{LM} compare better than L3O_L to L3L. However, there are 5 cases
737 where L3O_{LM} and L3L yield significantly different results. For 3 of these (Dubai, Hong Kong, and Istanbul),
738 interpretation of the difference is simple: L3O_{LM} is a significant under-estimate of the CO change over time,
739 likely due to the influence of retrievals over water on the dataset (L3W yields a significantly weaker trend
740 than L3L in all 3 cases). In the remaining 2 cases – New York and Saigon – interpretation is more
741 complicated. For both cities, the trend detected in L3L is not significantly different from zero, whereas the
742 trend in L3O_{LM} is. Does this mean that the trend in L3O_{LM} is an over-estimate? Possibly. However, in both
743 cases, the trends are within one standard error of each other and therefore within the range of sampling
744 uncertainty. There are an additional 2 cities where WLS could be performed in L3L but not L3O_{LM} (Dar Es
745 Salaam and Taipei), but $n_{\text{days}}(\text{L3L})$ is so low (44 and 36, respectively) that these results are not deemed to
746 be trustworthy.

747
748
749
750
751
752
753
754

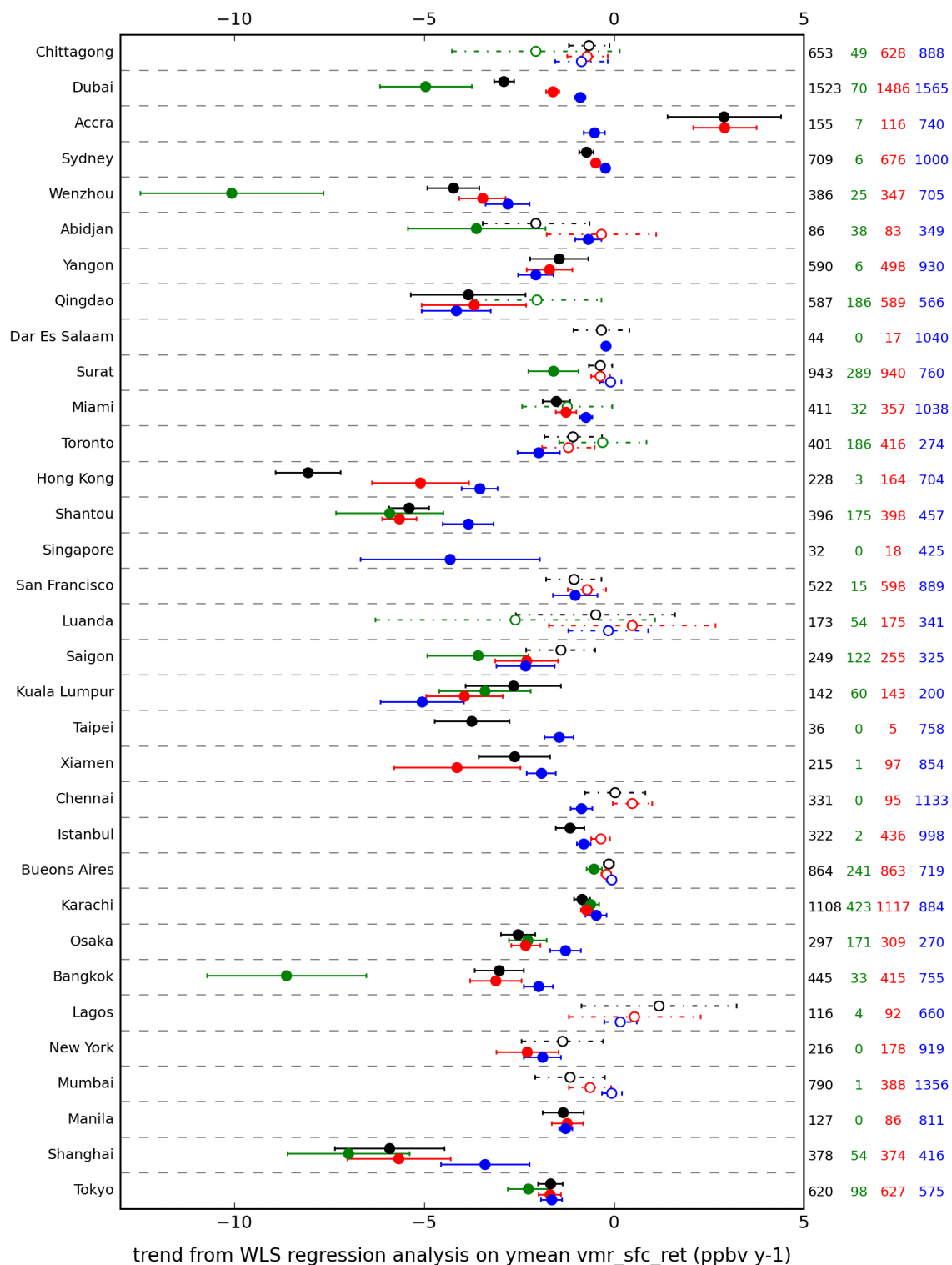




Figure 9. Comparison of temporal trend (detected using WLS, as outlined in Section 2.5) in retrieved surface level VMR in L3L (black), L3O_L (green), L3O_{LM} (red), and L3W (blue), for the 33 largest coastal cities (ordered by population on the y-axis). The trend value (in ppbv y⁻¹) is indicated by the filled/open circle on each row, and its standard error by the error bars. For all datasets, whether the marker is filled or not, and whether the lines are solid or dash/dot, depends on the significance of the trend: filled markers and solid lines indicate the trend is significant ($p < 0.1$); open markers and dash/dot lines indicate that the trend is not significantly different to zero. The number of retrieval days in each time series analysed for each city is given on the right-hand y-axis, color-coded according to dataset.

756

757 4. Summary and Conclusions

758

759 Motivated by the work of Ashpole and Wiacek (2020) which demonstrated, for the MOPITT L3 grid box
760 containing coastal city of Halifax, Canada, that mean VMR statistics and temporal trends differ depending
761 on whether L2 or L3 data are analysed, this paper has examined what proportion of all coastal L3 grid boxes
762 also see differences between results from analyses performed with L2 and L3 data. While it is recommended

763

764 to MOPITT data users that analyses are restricted to retrievals performed over land owing to known
765 sensitivity issues over water (MOPITT Algorithm Development Team, 2018; Deeter et al., 2015), such
766 recommendations cannot practically be followed by users of L3 data for coastal grid boxes owing to the way
767 the data are created from their bounded L2 retrievals. In short, this study has sought to answer the question:
768 “does it matter”? The main results are summarised below.

769 First, a direct comparison of the L2 retrievals performed over land (L3L) and water (L3W) that are
770 averaged together to create L3 products on days when the L3 surface index is “mixed” (L3O_M) identified
771 that:

772

773 • Retrieval information content is clearly greater in L3L than L3W. The mean L3L – L3W VMR
774 difference is over 10 ppbv, significant ($p < 0.1$) at 60 % of the coastal grid boxes compared. Temporal
775 trends are also stronger, on average, in L3L (mean diff = 0.28 ppbv y⁻¹, 0.43 ppbv y⁻¹ if only
776 considering trends significantly different to zero), with the L3L – L3W trend difference significant
777 ($p < 0.1$) at 36 % of grid boxes where a trend comparison was possible. The largest L3L – L3W
778 differences in mean VMRs and trends are clearly associated with greater differences in retrieval
779 sensitivity.

780 • The resulting VMRs in L3O_M are significantly different to L3L for 75 % of grid boxes where the
781 L3L – L3W difference is also significant; this corresponds to 45 % of all coastal grid boxes



782 compared. Whether or not $L3O_M$ and $L3L$ differ significantly depends on multiple factors including
783 the ratio of land/water surface cover in the grid box, the strength of the land-water sensitivity contrast
784 and VMR difference, and, potentially, the accuracy of the a priori. Just under half of the grid boxes
785 that featured a significant $L3L - L3W$ trend difference also see trends differing significantly between
786 $L3L$ and $L3O_M$. As with the mean VMR comparison, these grid boxes are more water-dominated
787 than the subset whereby the $L3L - L3W$ trend difference is significant but the $L3L - L3O_M$ trend
788 difference is not. They also feature stronger $L3L - L3W$ trend differences overall, but no other
789 variables (such as l_{tm} VMRs and sensitivity metrics) show clear differences.

790

791 Having established the degree of difference in $L3O_M$ and $L3L$ retrievals that is caused directly by
792 averaging $L3L$ with the less-sensitive $L3W$, the full $L3O$ dataset with differing surface filtering options was
793 compared to $L3L$:

794

- 795 • If $L3O$ is filtered so that only retrievals over land ($L3O_L$) are analysed, as has been recommended
796 (MOPITT Algorithm Development Team, 2018; Deeter et al., 2015), there is a huge loss of data, in
797 terms of days with data to analyse. This is a direct result of $L2$ retrievals over land routinely being
798 discarded during the $L3O$ creation process (at least for coastal grid boxes). The problem can be
799 alleviated by also retaining $L3O_M$ retrievals, but these additional days with data feature some
800 influence from retrievals made over water that can affect results, as outlined. The resulting $L3O_{LM}$
801 subset still has less days with data than in $L3L$ for 61 % of coastal grid boxes.
- 802 • Almost a quarter (half) of coastal grid boxes see a significant difference in l_{tm} VMR between $L3L$
803 and $L3O_L$ ($L3O_{LM}$). Over a third (almost a quarter) of the trends in $L3O_L$ ($L3O_{LM}$) are significantly
804 different to $L3L$.
- 805 • Focusing on the 33 largest coastal cities in the world, mean VMRs in $L3O_L$ and $L3L$ differ
806 significantly for 11 of the 27 cities that can be compared (40 %; there are no $L3O_L$ data for the
807 remaining 6 cities). The $L3L - L3O_{LM}$ mean VMR difference across all 33 cities is relatively small
808 (3.7 ppbv), but this does hide some much larger discrepancies, with the difference exceeding 10 ppbv
809 for 11 of the 33 cities and 20 ppbv for 3 of them. The difference is significant for 13 of 33 cities (39
810 %). Of the 18 cities where WLS analysis can be performed in $L3O_L$, there are 9 cases where the trend
811 is significantly different to that in $L3L$. The trends in $L3O_{LM}$ and $L3L$ differ significantly for 5 of the
812 33 cities.

813



814 From these results, it can be concluded that, yes, for at least a quarter of all MOPITT coastal L3 grid
815 boxes, it does matter that there is limited capacity to filter out the influence of retrievals over water in L3
816 data – at least without a huge loss of temporal coverage. Demonstrably, there are significant differences in
817 mean VMRs and temporal trends between L3O and L3L, sometimes very large. These differences could have
818 tangible consequences, depending on the purpose for which the MOPITT data are being used. While
819 acknowledging that this analysis has also shown that there is a sizeable proportion of coastal grid boxes where
820 statistically, mean VMRs and trends do not differ significantly between L3L and L3O, there is enough
821 evidence to support the suggestion from Ashpole and Wiacek (2020) that an additional L3 “land-only”
822 product, created only from averaging bounded L2 retrievals performed over land – the L3L dataset that has
823 been analysed in this paper – would be beneficial to the research community. This dataset would enable L3
824 users to maximize retrieval information content for coastal L3 grid boxes, as is currently only possible with
825 L2 data, while also preserving the benefits of L3 products. Although this analysis has focused only on analysis
826 of MOPITT data, it is reasonable to question whether the findings are applicable to data products from other
827 satellite instruments that make CO retrievals based on observed thermal-infrared radiances, such as AIRS
828 (Atmospheric InfraRed Sounder), TES (Tropospheric Emission Spectrometer), and IASI (Infrared
829 Atmospheric Sounding Interferometer).

830

831

832 **Data availability**

833

834 MOPITT data were downloaded from the NASA Earthdata portal (<https://search.earthdata.nasa.gov/>). The
835 L3L and L3W products analysed in this study are available on request from the corresponding author.

836

837

838 **Author contributions**

839

840 IA and AW jointly conceived of and designed the study. IA performed data analysis; both authors examined
841 and interpreted the results, and prepared the manuscript.

842

843

844 **Competing interests**

845

846 The authors declare that they have no conflict of interest.



847

848

849 **Acknowledgements**

850

851 The authors received funding from the Canadian Space Agency through the Earth System Science Data
852 Analyses program (grant no. 16SUASMPN), the Canadian National Science and Engineering Research
853 Council through the Discovery Grants Program, and Saint Mary's University. We thank the MOPITT team
854 for providing the data used in this study.

855

856

857 **References**

858

859 Ashpole, I., & Wiacek, A.: Impact of land-water sensitivity contrast on MOPITT retrievals and trends over
860 a coastal city, *Atmospheric Measurement Techniques*, 13(7), 3521–3542, <https://doi.org/10.5194/amt-13-3521-2020>, 2020.

862 Buchholz, R. R., Worden, H. M., Park, M., Francis, G., Deeter, M. N., Edwards, D. P., Emmons, L. K.,
863 Gaubert, B., Gille, J., Martínez-Alonso, S., Tang, M., Kumar, R., Drummond, J. R., Clerbaux, C., George,
864 M., Coheur, P-F., Hurtmans, D., Bowman, K. W., Luo, M., Payne, V. H., Worden, J. R., Chin, M., Levy,
865 R. C., Warner, J., Wei, Z., Kulawik, S. S.: Air pollution trends measured from Terra: CO and AOD over
866 industrial, fire-prone, and background regions, *Remote Sensing of Environment*, 256, 112275,
867 <https://doi.org/10.1016/j.rse.2020.112275>, 2021.

868 Deeter, M. N., Emmons, L. K., Francis, G. L., Edwards, D. P., Gille, J. C., Warner, J. X., Khattatov, B.,
869 Ziskin, D., Lamarque, J.-F., Ho, S.-P., Yudin, V., Attié, J.-L., Packman, D., Chen, J., Mao, D. Drummond,
870 J. R.: Operational carbon monoxide retrieval algorithm and selected results for the MOPITT instrument,
871 *Journal of Geophysical Research*, 108(D14), 4399, <https://doi.org/10.1029/2002JD003186>, 2003.

872 Deeter, M. N., Edwards, D. P., Gille, J. C., and Drummond, J. R.: Sensitivity of MOPITT observations to
873 carbon monoxide in the lower troposphere, *Journal of Geophysical Research Atmospheres*, 112(24), 1–9,
874 <https://doi.org/10.1029/2007JD008929>, 2007.

875 Deeter, M. N., Martínez-Alonso, S., Edwards, D. P., Emmons, L. K., Gille, J. C., Worden, H. M., Pittman, J.
876 V., Daube, B. C. and Wofsy, S. C.: Validation of MOPITT Version 5 thermal-infrared, near-infrared, and
877 multispectral carbon monoxide profile retrievals for 2000–2011, *Journal of Geophysical Research*
878 *Atmospheres*, 118(12), 6710–6725, <https://doi.org/10.1002/jgrd.50272>, 2013.



- 879 Deeter, M. N., Martínez-Alonso, S., Edwards, D. P., Emmons, L. K., Gille, J. C., Worden, H.M., Sweeney,
880 C., Pittman, J. V., Daube, B. C., and Wofsy, S. C.: The MOPITT Version 6 product: Algorithm
881 enhancements and validation, *Atmospheric Measurement Techniques*, 7(11), 3623–3632,
882 <https://doi.org/10.5194/amt-7-3623-2014>, 2014.
- 883 Deeter, M. N., Edwards, D. P., Gille, J. C., and Worden, H. M.: Information content of MOPITT CO profile
884 retrievals: Temporal and geographical variability, *Journal of Geophysical Research: Atmospheres*,
885 120(24), 12723–12738, <https://doi.org/10.1002/2015JD024024>, 2015.
- 886 Deeter, M. N., Edwards, D. P., Francis, G. L., Gille, J. C., Mao, D., Martínez-Alonso, S., Worden, H.M,
887 Ziskin, D., and Andreae, M. O.: Radiance-based retrieval bias mitigation for the MOPITT instrument:
888 The version 8 product, *Atmospheric Measurement Techniques*, 12(8), 4561–4580,
889 <https://doi.org/10.5194/amt-12-4561-2019>, 2019.
- 890 Deeter, M., Francis, G., Gille, J., Mao, D., Martínez-Alonso, S., Worden, H., Ziskin, D., Drummond, J.,
891 Commane, R., Diskin, G., and McKain, K.: The MOPITT Version 9 CO Product: Sampling Enhancements
892 and Validation, *Atmos. Meas. Tech. Discuss.* [preprint], <https://doi.org/10.5194/amt-2021-370>, in review,
893 2021.
- 894 Drummond, J. R., Zou, J., Nichitiu, F., Kar, J., Deschambaut, R., and Hackett, J.: A review of 9-year
895 performance and operation of the MOPITT instrument, *Advances in Space Research*, 45(6), 760–774,
896 <https://doi.org/10.1016/j.asr.2009.11.019>, 2010.
- 897 Drummond, J. R., Hackett, J., and Caldwell, D.: Measurements of pollution in the troposphere (MOPITT),
898 in: *Optical Payloads for Space Missions*, edited by: Shen-En Qian, Wiley and Sons, West Sussex, UK,
899 639–652, 2016.
- 900 Duncan, B. N., Logan, J. A., Bey, I., Megretskaia, I. A., Yantosca, R. M., Novelli, P. C., Jones, N.B., and
901 Rinsland, C. P.: Global budget of CO, 1988 - 1997: Source estimates and validation with a global model,
902 *Journal of Geophysical Research Atmospheres*, 112(22), D22301, <https://doi.org/10.1029/2007JD008459>,
903 2007.
- 904 Edwards, D. P., Halvorson, C. M., and Gille, J. C.: Radiative transfer modeling for the EOS Terra satellite
905 Measurement of Pollution in the Troposphere (MOPITT) instrument, *Journal of Geophysical Research*
906 *Atmospheres*, <https://doi.org/10.1029/1999JD900167>, 1999.
- 907 Francis, G. L., Deeter, M. N., Martínez-Alonso, S., Gille, J. C., Edwards, D. P., Mao, D., Worden, H. M.,
908 and Ziskin, D.: Measurement of Pollution in the Troposphere Algorithm Theoretical Basis Document:
909 Retrieval of Carbon Monoxide Profiles and Column Amounts from MOPITT Observed Radiances (Level
910 1 to Level 2), *Atmospheric Chemistry Observations and Modelling Laboratory, National Center for*



- 911 Atmospheric Research, Boulder, Colorado, downloaded from:
912 https://www2.acom.ucar.edu/sites/default/files/mopitt/ATBD_5_June_2017.pdf, 2017.
- 913 Hedelius, J. K., Toon, G. C., Buchholz, R. R., Iraci, L. T., Podolske, J. R., Roehl, C. M., Wennberg, P. O.,
914 Worden, H. M., Wunch, D.: Regional and Urban Column CO Trends and Anomalies as Observed by
915 MOPITT Over 16 Years, *Journal of Geophysical Research: Atmospheres*, 126(5), 1–18,
916 <https://doi.org/10.1029/2020JD033967>, 2021.
- 917 Lamarque, J. F., Emmons, L. K., Hess, P. G., Kinnison, D. E., Tilmes, S., Vitt, F., Heald, C. L., Holland, E.
918 A., Lauritzen, P. H., Neu, J., Orlando, J. J., Rasch, P. J., and Tyndall, G. K.: CAM-chem: Description and
919 evaluation of interactive atmospheric chemistry in the Community Earth System Model, *Geoscientific*
920 *Model Development*, 5(2), 369–411, <https://doi.org/10.5194/gmd-5-369-2012>, 2012.
- 921 MOPITT Algorithm Development Team: MOPITT (Measurements of Pollution in the Troposphere) Version
922 8 Product User’s Guide, Atmospheric Chemistry Observations and Modeling Laboratory, National Center
923 for Atmospheric Research, Boulder, downloaded from:
924 https://www2.acom.ucar.edu/sites/default/files/mopitt/v8_users_guide_201812.pdf, 2018.
- 925 Pan, L., Edwards, D. P., Gille, J. C., Smith, M. W., and Drummond, J. R.: Satellite remote sensing of
926 tropospheric CO and CH₄: forward model studies of the MOPITT instrument, *Applied Optics*, 34(30),
927 6976. <https://doi.org/10.1364/ao.34.006976>, 1995.
- 928 Pan, L., Gille, J. C., Edwards, D. P., Bailey, P. L., and Rodgers, C. D.: Retrieval of tropospheric carbon
929 monoxide for the MOPITT experiment, *Journal of Geophysical Research*, 103(D24), 32277.
930 <https://doi.org/10.1029/98JD01828>, 1998.
- 931 Rodgers, C. D.: *Inverse Methods for Atmospheric Sounding, Theory and Practice*, World Scientific,
932 Singapore, 2000.
- 933 Worden, H. M., Deeter, M. N., Edwards, D. P., Gille, J. C., Drummond, J. R., and Nédélec, P.: Observations
934 of near-surface carbon monoxide from space using MOPITT multispectral retrievals, *Journal of*
935 *Geophysical Research Atmospheres*, 115(18), 1–12, <https://doi.org/10.1029/2010JD014242>, 2010.
- 936 Worden, H. M., Deeter, M. N., Edwards, D. P., Gille, J., Drummond, J., Emmons, L. K., Francis, G., and
937 Martínez-Alonso, S.: 13 years of MOPITT operations: Lessons from MOPITT retrieval algorithm
938 development, *Annals of Geophysics*, 56(FAST TRACK 1), 1–5, <https://doi.org/10.4401/ag-6330>, 2014.